

# A Stackelberg Game Model for Overlay D2D Transmission With Heterogeneous Rate Requirements

Jiangbin Lyu, Yong Huat Chew, *Member, IEEE*, and Wai-Choong Wong, *Senior Member, IEEE*

**Abstract**—This paper studies the performance of overlay device-to-device (D2D) communication links via carrier-sense multiple access (CSMA) protocols. We assume that the D2D links have heterogeneous rate requirements and different willingness to pay, and each of them acts nonaltruistically to achieve its target rate while maximizing its own payoff. Spatial reuse is allowed if the links are not interfering with each other. A noncooperative game model is used to address the resource allocation among the D2D links, at the same time leveraging on the ideal CSMA network (ICN) model to address the physical channel access issue. We propose a Stackelberg game in which the base station (BS) in the cellular network acts as a Stackelberg leader to regulate the individual payoff by modifying the unit service price so that the total D2D throughput is maximized. The problem is shown to be quasi-convex and can be solved by a sequence of equivalent convex optimization problems. The pricing strategies are designed so that the network always operates within the feasible throughput region. The results are verified by simulations.

**Index Terms**—Device-to-device (D2D) communications, game theory, heterogeneous traffic, spatial carrier-sense multiple access (CSMA), transmission aggressiveness (TA).

## I. INTRODUCTION

THE growing popularity of smartphones and tablets has resulted in the increasing demand for high-data-rate services, and a huge amount of data traffic normally needs to be transmitted through cellular networks, which in turn leads to severe traffic overload problems. Recently, device-to-device (D2D) communication has emerged as a new data-offloading solution by enabling direct communication between two mobile users without traversing the base station (BS) [1].

D2D communication can be implemented over the cellular spectrum (i.e., in-band) or the unlicensed spectrum (i.e., out-

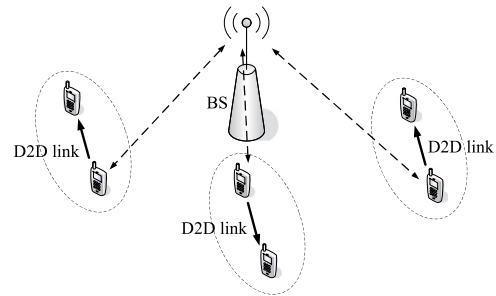


Fig. 1. Example of overlay D2D communications. (Solid arrow) Data communication of a D2D link. (Dashed arrow) Control information exchange between a D2D transmitter and the BS.

band). In-band D2D can be further classified into spectrum overlay and spectrum underlay. In the overlay scenario, the cellular and D2D transmitters use orthogonal time/frequency resources, whereas in the underlay scenario, the D2D transmitters access the same time/frequency resources occupied by cellular users. The rate performance is evaluated in [2] for both overlay and underlay scenarios. It is observed that D2D mobiles in both scenarios can enjoy much higher data rates than regular cellular mobiles. As for cellular mobiles in the overlay scenario, their rate performance also improves due to the offloading capability of D2D communication. In addition to performance improvement over the pure cellular mode, in-band overlay D2D is also more tractable in analysis since it does not interfere with regular cellular mobiles or suffer from random interference from unlicensed band.

In [2], the authors use a simple spatial Aloha access scheme to support D2D scheduling. In this paper, we assume that all D2D links use carrier-sense multiple access (CSMA) as the multiple access scheme to share a dedicated in-band overlay channel. Spatial reuse is considered, i.e., different transmit-receive (Tx-Rx) pairs at a sufficient distance away that do not cause interference are allowed to transmit simultaneously [3]. Although D2D communication does not route the data traffic through the cellular network, the available network infrastructure can be still an effective means to exert light control over all the D2D links when performing resource allocation. In our model, the D2D links have heterogeneous service requirements and different willingness to pay, and the central entity (e.g., evolved node B) [1] controls the transmission behaviors of all links by modifying the price per unit service rate. A simple example is given in Fig. 1, where there

Manuscript received March 24, 2015; revised August 19, 2015 and October 14, 2015; accepted December 13, 2015. Date of publication December 24, 2015; date of current version October 13, 2016. This work was carried out at the Sensor-Enhanced Social Media (SeSaMe) Centre. It was supported by the Singapore National Research Foundation under its IRC@SG Funding Initiative and administered by the Interactive and Digital Media Programme Office. The review of this paper was coordinated by Prof. Y. Qian.

J. Lyu and W.-C. Wong are with the Department of Electrical and Computer Engineering, National University of Singapore, Singapore 117583 (e-mail: jiangbin.lu@u.nus.edu; elewwcl@nus.edu.sg).

Y. H. Chew is with the Institute for Infocomm Research (I<sup>2</sup>R), Agency for Science, Technology and Research, Singapore 138632 (e-mail: chewyh@i2r.a-star.edu.sg).

Color versions of one or more of the figures in this paper are available online at <http://ieeexplore.ieee.org>.

Digital Object Identifier 10.1109/TVT.2015.2511924

are three D2D links, and a single BS oversees/controls them in the control plane. Each D2D link consists of a Tx–Rx pair, and hence, the D2D links resemble the situation where distributed pairs are transmitting. Hereafter, the terms “D2D link,” “CSMA Tx–Rx pair,” and “CSMA user” are used synonymously. The involvement of the cellular network in the control plane is the key difference between our system model with that defined in Mobile Ad hoc NETworks (MANETs) [4]. Moreover, D2D communication is mainly used for single-hop communications, which does not inherit the multihop routing problem of MANETs and wireless sensor networks [5].

When spatial reuse is considered in CSMA methods, the carrier-sense relationships among the CSMA users become *non-all-inclusive*, i.e., each CSMA user may sense only a subset but not all other users. As commented by Liew *et al.* [3], it is extremely difficult to extend the analytic methods for all-inclusive carrier-sense networks (e.g., [6]–[8]) to the non-all-inclusive case because of the inhomogeneity in the state spaces of the CSMA users. In fact, the problem of computing user throughputs in a spatial CSMA network is shown to be NP-hard [3]. To perform tractable analysis, existing studies [3], [9]–[11] have adopted an *ideal CSMA network (ICN)* model to capture the essence of the CSMA mechanism under spatial reuse. In this paper, we also leverage the ICN model to address the physical channel access issue.

Our contributions in this paper are twofold. First, we propose a Stackelberg game [12] that maximizes the total throughput of the D2D links, where these links have heterogeneous utility functions. The BS in the cellular networks will act as a Stackelberg leader to regulate the D2D link transmissions by modifying the service price so that the payoff of each individual D2D link can be maximized while maintaining the D2D network to function within the feasible throughput region determined by the CSMA mechanism. The problem is shown to be quasi-convex and can be solved by a sequence of equivalent convex optimization problems. The pricing strategies are designed so that the network always operates within the feasible throughput region. Second, each D2D link will acquire a rate based on its actual demand and willingness to pay. We explicitly model the possible selfish behaviors among the D2D links with spatial reuse. Under a given network price, the transmitter of each D2D link competes for channel usage by choosing its transmission parameters to maximize its own payoff. Such user dynamics are studied in the setting of noncooperative games, and the resulting CSMA game model serves as the follower subgame in the proposed Stackelberg game. An algorithm is proposed followed by proofs for the existence and convergence of the equilibrium solution.

The remainder of this paper is organized as follows. We introduce related works in Section II and the network model in Section III, and summarize some important results on the ICN. In Section IV, the feasible throughput region for a CSMA network is defined, whereas some important properties are derived. The Stackelberg game is detailed in Section V. The performance of the proposed game is evaluated through simulations in Section VI. We conclude this paper in Section VII.

The notations used in this paper are as follows. An arrow over a variable  $\vec{\cdot}$  represents a vector or a system state consisting of the

binary status of the  $N$  links. Variable  $\theta$  denotes the throughput from the channel access point of view, where the solution is controlled by the ICN model. On the other hand,  $\tilde{\theta}$  represents a desired throughput from the link layer aspect, whose value is derived from the price and link utility function. If the final solution is within the feasible throughput region, these two values should match. There are two types of equilibriums to be differentiated: The subgame equilibrium is denoted by superscript “\*,” whereas the equilibrium for the Stackelberg game is denoted by superscript “opt.”

## II. RELATED WORKS

### A. Spectrum Sharing Games for D2D Communication

In the licensed spectrum, a potential D2D pair can communicate through conventional cellular mode (relay through the BS), dedicated D2D mode (spectrum overlay), or underlay sharing mode (share with cellular users). Game-theoretic approaches have been applied in D2D communications for mode selection and resource management [13]. In particular, Cai *et al.* [14] model the spectrum sharing mode selection as a coalition formation game and propose a distributed coalition formation algorithm to improve the total achievable rate. Wu *et al.* [15] study the underlay spectrum sharing problem among potential D2D pairs and cellular users with quality-of-service requirements. A coalition formation game and a distributed coalition formation algorithm are proposed to decide on the most energy-efficient spectrum sharing strategy. The focus of these studies is to look for efficient spectrum sharing solutions among the D2D pairs and cellular users, and spectrum underlay is adopted in the sharing mode under the constraints on the amount of mutual interference. In this paper, we focus on spectrum overlay mode, in which the number of orthogonal channels is limited and multiple D2D pairs share a common channel via distributed transmission scheduling.

### B. CSMA Distributed Transmission Scheduling

A survey on applying game theory to CSMA can be found in [16], where several noncooperative contention control games in CSMA methods are presented. For example, Jin and Kesidis [17] analyze the noncooperative user behaviors in CSMA wireless networks where users have the freedom to choose the contention window sizes according to the network congestion level. The existence and uniqueness of the equilibrium point are investigated, as well as a distributed iterative method to approach the equilibrium. However, as stated in [16], most of the proposed CSMA games assume all-inclusive carrier sensing. The analysis cannot be directly applied in the presence of spatial reuse.

The ICN model captures the essence of spatial reuse CSMA networks. Jiang and Walrand [11] developed an elegant distributed CSMA algorithm for throughput and total utility maximization based on the ICN model after making assumptions about concavity and monotonicity of the user utility functions. Their work removes the need for knowledge of the underlying link topology, and their transmission parameters can be updated distributively. However, the approach implicitly assumes a best

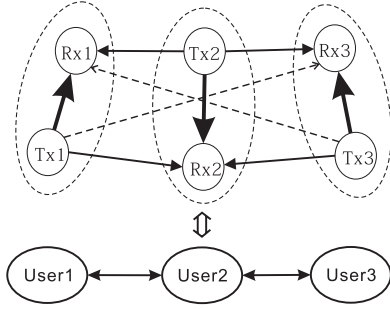


Fig. 2. Three Tx-Rx pairs and the corresponding contention graph [22]. In the upper part of the figure, the solid thick arrow represents the transmission link from a transmitter to its designated receiver; the solid thin and the dash thin arrows represent the nonnegligible and negligible interference, respectively.

effort transmission to achieve total utility maximization, and there is no explicit treatment if users have heterogeneous rate requirements and different willingness to pay. In other words, while optimizing the sum rate, there is no mechanism to weigh the individual user utility to differentiate the services. Moreover, the global optimization approach does not reflect the fact that users are selfish and behave nonaltruistically in maximizing their own payoffs. In fact, *Çagalj et al.* have shown that even the presence of a few selfish users may lead such a CSMA network to collapse [18], whereas proper pricing or penalty mechanisms lead to overall improvement [19]. Indeed, when users with heterogeneous rate requirements coexist in the network and the collective target rates are outside the feasible throughput region, the self-interested actions by the CSMA users would lead the network into heavily congested status. In this paper, we incorporate a game-theoretic framework into the ICN model to harness the selfish behaviors of a group of noncooperative spatially distributed CSMA users with heterogeneous rate requirements.

### III. SPATIAL REUSE CARRIER SENSE MULTIPLE ACCESS NETWORK

#### A. Spatial Reuse and Contention Graph

Assume that there are  $N$  D2D links in the network that share a dedicated in-band overlay channel via CSMA-like random access. These D2D links can transmit in the same frequency band simultaneously if they do not cause any performance degradation to each other. We assume that the CSMA network is hidden-node-free, which can be achieved by properly setting the carrier-sensing power threshold as in [20] and [21]. Such a spatial reuse model can be characterized by a “contention graph” as in [3]. For simplicity, only a connected network is considered, and if the network is not connected, then it can be divided into several independent connected subnetworks and dealt with separately. We assume that the contention graph is undirected and the transmission queue of each D2D link is continuously backlogged, i.e., the transmitter of every D2D link always has a packet to transmit to its designated receiver. An example for three D2D links is shown in Fig. 2, where D2D links 1 and 3 can concurrently transmit without collisions, but neither of them can transmit together with link 2. In such cases, link 2 is a neighbor of link 1, but link 3 is not.

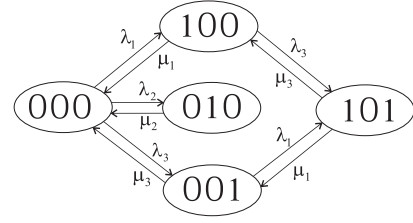


Fig. 3. State transition diagram for Fig. 2.

#### B. ICN Model

In the CSMA random access method, a link senses the channel before transmitting. Based on such a carrier-sensing relationship, a link will refrain from transmitting if any of its neighbors is transmitting. In the ICN model, each link maintains a countdown timer whose value  $t_{cd}$  is modeled as a continuous random variable with an arbitrary distribution [3]. The timer value  $t_{cd}$  counts down if the channel is sensed as idle and is frozen if the channel is sensed as busy. When the channel becomes idle again, the countdown of  $t_{cd}$  resumes until  $t_{cd} = 0$ , upon which the link transmits a packet. The transmission time  $t_{tr}$  is a random variable with an arbitrary distribution. For simplicity, we have adopted uniform distributions for both  $t_{cd}$  and  $t_{tr}$  in our simulations.

At any time, a link is either transmitting or idle. Denote the state of link  $i$  as  $s_i \in \{0, 1\}$ , where  $s_i = 1$  if link  $i$  is transmitting; otherwise,  $s_i = 0$ . When  $s_i = 0$ , link  $i$  is either actively counting down or frozen, depending on whether a neighboring link  $j$  is transmitting. We shall denote the system state of an  $N$ -link ICN by an  $N$ -tuple binary vector  $\vec{s} = [s_1, s_2, \dots, s_N]$  or simply by a string  $s_1 s_2, \dots, s_N$ . Notice that  $s_i = s_j = 1$  is not allowed if links  $i$  and  $j$  are neighbors for the reasons that they can sense each other, and the probability of them counting down to zero simultaneously is negligibly small under ICN due to the adopted continuous random variables [3]. Therefore, each feasible state corresponds to an independent set [3] of the contention graph.

For the example in Fig. 2, the five independent sets are  $\emptyset$ ,  $\{1\}$ ,  $\{2\}$ ,  $\{3\}$ , and  $\{1, 3\}$ . By default, we also include  $\emptyset$ , which corresponds to  $\vec{s} = \vec{0}$ , as an independent set. The collection of these feasible system states is denoted by the set

$$\mathcal{S} = \{[0, 0, 0], [1, 0, 0], [0, 1, 0], [0, 0, 1], [1, 0, 1]\}. \quad (1)$$

If we denote the state  $\vec{s}$  with  $s_j = 0 \forall j \in \mathcal{N} = \{1, 2, \dots, N\}$  as  $\vec{e}_0$  and the state  $\vec{s}$  with  $s_i = 1, s_j = 0 \forall j \neq i$  as  $\vec{e}_i$ , then  $\mathcal{S}$  can be denoted as

$$\mathcal{S} = \{\vec{e}_0, \vec{e}_1, \vec{e}_2, \vec{e}_3, \vec{e}_1 + \vec{e}_3\}. \quad (2)$$

#### C. Stationary Distribution

Here, we summarize the stationary distribution of the system states based on the results in [3]. If the transmission time and countdown time are exponentially distributed, then the system state  $\vec{s}(t)$  is a time-reversible Markov process. The state transition diagram of the example in Fig. 2 is shown in Fig. 3,

where there are five feasible system states. Each transition, from a state in the left to a state in the right, represents the beginning of a link transmission, whereas the reverse transition represents the ending of the same link transmission. For example, the transition from 001 to 101 represents the beginning of link 1's transmission while link 3 is transmitting. Similarly, the transition from 101 to 001 represents the ending of link 1's transmission while link 3 continues its transmission.

The transition rate of a link from idle state to transmission state is  $\lambda = 1/E[t_{cd}]$ , whereas the transition rate from transmission state to idle state is  $\mu = 1/E[t_{tr}]$ . Hence, a higher rate  $\lambda$  and a lower rate  $\mu$  suggest a higher intensity of the link to access the channel. We define the *access intensity* (AI) [3] of a link as the ratio of its mean transmission time to its mean countdown time:  $\rho = E[t_{tr}]/E[t_{cd}] = \lambda/\mu$ . Note that a higher value of AI suggests a higher intensity to access the channel. We further define the *transmission aggressiveness* (TA) [11], which is the natural logarithm of AI  $\rho$ , i.e.,  $r = \log_e \rho$ . Since natural logarithm is a monotonically increasing function, a higher value of AI corresponds to a higher value of TA, which suggests that the link is more aggressive to transmit.

Given a profile of AIs  $\vec{\rho} = [\rho_1, \rho_2, \dots, \rho_N]$ , the stationary probability of the state  $\vec{s} \in \mathcal{S}$  is shown in [3] to be given by

$$p_{\vec{s}} = 1/Z \cdot \prod_{i:s_i=1} \rho_i \quad \forall \vec{s} \in \mathcal{S} \quad (3)$$

where

$$Z = \sum_{\vec{s} \in \mathcal{S}} \prod_{i:s_i=1} \rho_i \quad (4)$$

and by default,  $p_{\vec{e}_0} = 1/Z$ . In (4), when evaluating  $p_{\vec{s}}$ , the notation  $\prod_{i:s_i=1} \rho_i$  means that, for each state  $\vec{s}$ , only those transmitting links are involved in the multiplication. Collectively, we can write the state probability distribution as a vector  $\vec{p} = [p_{\vec{s}_1}, p_{\vec{s}_2}, \dots, p_{\vec{s}_{|\mathcal{S}|}}]$ , where  $|\mathcal{S}|$  is the cardinality of the set  $\mathcal{S}$ , i.e., the number of feasible states.

Similarly, if we replace AIs by TAs and define a profile of TAs  $\vec{r} = [r_1, r_2, \dots, r_N] = \log_e \vec{\rho}$  for all links, the stationary state probabilities are given by

$$p_{\vec{s}} = 1/Z \cdot \exp \left( \sum_{i=1}^N s_i r_i \right) \quad \forall \vec{s} \in \mathcal{S} \quad (5)$$

where

$$Z = \sum_{\vec{s} \in \mathcal{S}} \exp \left( \sum_{i=1}^N s_i r_i \right). \quad (6)$$

As an illustration, consider the state transition diagram in Fig. 3. Since the system state is a time-reversible Markov process, the stationary probability distribution should satisfy

$$\begin{cases} p_{100} = \rho_1 \cdot p_{000} \\ p_{010} = \rho_2 \cdot p_{000} \\ p_{001} = \rho_3 \cdot p_{000} \\ p_{101} = \rho_1 \cdot p_{001} = \rho_3 \cdot p_{100} = \rho_1 \cdot \rho_3 \cdot p_{000} \\ p_{000} + p_{100} + p_{010} + p_{001} + p_{101} = 1. \end{cases} \quad (7)$$

Solving the equations in (7) yields

$$p_{000} = \frac{1}{(1 + \rho_1 + \rho_2 + \rho_3 + \rho_1 \rho_3)} = \frac{1}{Z} \quad (8)$$

where  $Z$  is given in (4). Once  $Z$  is evaluated, other state probabilities can be easily computed.

Despite the idealized assumption about instantaneous sensing and continuous backoff time, the ICN model does capture the essence of CSMA under spatial reuse. It is shown in [3] that the stationary probability distribution in (3) holds even if both the transmission time and the countdown time are not exponentially distributed, given that the ratio of their mean  $\rho_i = E[t_{tr,i}]/E[t_{cd,i}]$  for each link  $i \in \mathcal{N}$  remains unchanged. On the other hand, in the discrete time model, the stationary probability distribution will deviate from (3) due to collisions. Fortunately, when request-to-send/clear-to-send handshaking is used and under the same TA, the stationary distribution will approach that given in (3) since the collision period will be comparatively small for a sufficiently large holding time [23].

Finally, it then follows from (5) and (6) that the throughput or mean service rate of link  $i$  is given by

$$\theta_i = \sum_{\vec{s} \in \mathcal{S}} s_i p_{\vec{s}} = \frac{\sum_{\vec{s} \in \mathcal{S}} s_i \exp \left( \sum_{i=1}^N s_i r_i \right)}{\sum_{\vec{s} \in \mathcal{S}} \exp \left( \sum_{i=1}^N s_i r_i \right)} \quad \forall i \in \mathcal{N} \quad (9)$$

which is the sum of the stationary state probabilities defined in (5) in which link  $i$  is actively transmitting (i.e.,  $s_i = 1$ ). In vector form, if we define the vector  $\vec{\theta} = [\theta_1, \theta_2, \dots, \theta_N]$ , then the  $N$  equations in (9) can be collectively written as

$$\vec{\theta} = \sum_{\vec{s} \in \mathcal{S}} p_{\vec{s}} \vec{s} \quad (10)$$

where  $\vec{s}$  is the  $N$ -dimensional vector used to represent a system state.

#### IV. FEASIBLE THROUGHPUT REGION IN SPATIAL CARRIER SENSE MULTIPLE ACCESS NETWORKS

Here, we state and derive the key results on ICN, which are important to our proposed game-theoretic framework presented in Section V.

##### A. Feasible and Strictly Feasible Throughput Region

Each feasible system state  $\vec{s} \in \mathcal{S}$  corresponds to a feasible scheduling vector of link transmissions. The feasible throughput region is therefore the convex hull [24, p. 24] of  $\mathcal{S}$ , i.e.,

$$\bar{\mathcal{C}} = \left\{ \vec{\theta} \mid \vec{\theta} = \sum_{\vec{s} \in \mathcal{S}} p_{\vec{s}} \vec{s} \wedge (p_{\vec{s}} \geq 0 \quad \forall \vec{s}) \wedge \left( \sum_{\vec{s} \in \mathcal{S}} p_{\vec{s}} = 1 \right) \right\}. \quad (11)$$

Equation (11) shows that the feasible solutions are given by the convex combinations of the throughputs at these feasible states while fulfilling the probability and probability distribution constraints. The solutions are fully defined by a polytope whose vertices are the feasible system states  $\vec{s} \in \mathcal{S}$ .

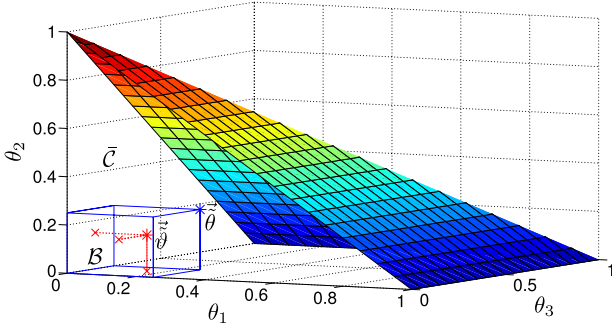


Fig. 4. Feasible throughput region for the contention graph in Fig. 2.

The interior of  $\bar{\mathcal{C}}$  is the *strictly feasible region*  $\mathcal{C}$

$$\mathcal{C} = \left\{ \bar{\theta} \left( \bar{\theta} = \sum_{\vec{s} \in \mathcal{S}} p_{\vec{s}} \vec{s} \right) \wedge (p_{\vec{s}} > 0 \forall \vec{s}) \wedge \left( \sum_{\vec{s} \in \mathcal{S}} p_{\vec{s}} = 1 \right) \right\}. \quad (12)$$

Using the contention graph in Fig. 2 as an example, the set of feasible system states  $\mathcal{S}$  has been given in (1). The feasible throughput region is  $\bar{\mathcal{C}}$ , as shown in Fig. 4, which is a polyhedron vertexed by the maximum throughput of these states (the region enclosed by the mesh surface and its intersections with  $\theta_1 - \theta_2$ ,  $\theta_1 - \theta_3$ , and  $\theta_2 - \theta_3$  planes). The strictly feasible region  $\mathcal{C}$  refers to the inner region of the polyhedron only.

### B. Transmission Aggressiveness

CSMA is a distributed and randomized way to schedule the transmissions among the feasible system states. It is shown in [11] that by using the ICN model any throughput in the strictly feasible region can be achieved through a properly chosen TA  $\vec{r}$ , which is stated in the following lemma.

**Lemma 1** [25, Lemma 8]: In the ICN model, for any desired throughput for all the  $N$  links  $\vec{\theta} = [\tilde{\theta}_1, \tilde{\theta}_2, \dots, \tilde{\theta}_N] \in \mathcal{C}$  (strictly feasible region), there exists a unique finite-valued  $\vec{r} = [r_1, r_2, \dots, r_N] \in \mathcal{R}^N$  such that  $\theta_i(\vec{r}) = \tilde{\theta}_i \forall i \in \mathcal{N}$ .

A detailed proof can be found in [11] and [25]. Here, we only present a sketch of the proof.

*Proof:* Given a  $\vec{\theta} \in \mathcal{C}$ , we use the maximum log-likelihood method to estimate the parameters  $\vec{r}^*$  that result in  $\bar{\theta}(\vec{r}^*) = \vec{\theta}$  or, equivalently, result in the desired state probability distribution  $\vec{p}^{\bar{\theta}}$  such that  $\bar{\theta}(\vec{r}^*) = \sum_{\vec{s} \in \mathcal{S}} p_{\vec{s}}^{\bar{\theta}} \vec{s}$ . The log-likelihood function [26] is defined as

$$F(\vec{r}; \bar{\theta}) = \sum_{\vec{s} \in \mathcal{S}} p_{\vec{s}}^{\bar{\theta}} \log_e(p_{\vec{s}}). \quad (13)$$

By applying  $\bar{\theta} = \sum_{\vec{s} \in \mathcal{S}} p_{\vec{s}}^{\bar{\theta}} \vec{s}$  and substituting the expression for  $p_{\vec{s}}$  given in (5) and after some manipulations, we have

$$F(\vec{r}; \bar{\theta}) = \sum_{i=1}^N \tilde{\theta}_i r_i - \log_e \left[ \sum_{\vec{s} \in \mathcal{S}} \exp \left( \sum_{i=1}^N s_i r_i \right) \right]. \quad (14)$$

Since  $\sum_{i=1}^N \tilde{\theta}_i r_i$  is affine in  $\vec{r}$  and  $\log_e[\sum_{\vec{s} \in \mathcal{S}} \exp(\sum_{i=1}^N s_i r_i)]$  is a log-sum-exp function and thus is convex in  $\vec{r}$ , function  $F(\vec{r}; \bar{\theta})$  is concave in  $\vec{r}$  [24, p. 72]. Therefore, the subsequent

max-log-likelihood problem is a convex optimization problem with  $\vec{r}$  as the variables to be solved and  $\vec{\theta}$  as the parameters

$$\max_{\vec{r}} F(\vec{r}; \bar{\theta}) \quad (\text{Maximize log-likelihood}). \quad (15)$$

It is then shown in [11] that the max-log-likelihood problem in (15) is the dual problem of the max-entropy problem in (16), where  $-\sum_{\vec{s} \in \mathcal{S}} p_{\vec{s}} \log_e p_{\vec{s}}$  is the entropy of the distribution vector  $\vec{p}$  whose element  $p_{\vec{s}}$  is the state probability for the state  $\vec{s} \forall \vec{s} \in \mathcal{S}$ . The max-entropy problem is also a convex optimization problem, with  $\vec{p}$  as the variables and  $\vec{\theta}$  as the parameters

$$\begin{aligned} \max_{\vec{p}} \quad & -\sum_{\vec{s} \in \mathcal{S}} p_{\vec{s}} \log_e p_{\vec{s}} \quad (\text{Maximize entropy}) \\ \text{s.t.} \quad & \begin{cases} \sum_{\vec{s} \in \mathcal{S}} s_i p_{\vec{s}} = \tilde{\theta}_i \forall i \in \mathcal{N} \\ p_{\vec{s}} \geq 0 \forall \vec{s} \in \mathcal{S} \\ \sum_{\vec{s} \in \mathcal{S}} p_{\vec{s}} = 1. \end{cases} \end{aligned} \quad (16)$$

We are now ready to prove Lemma 1. We need to verify that Slater's condition [24, p. 226] is satisfied so that the optimal solutions to the two convex optimization problems (15) and (16) exist with zero duality gap, given that  $\vec{\theta} \in \mathcal{C}$  (strictly feasible region).

Since all the constraints in (16) are linear equalities and inequalities, we need to only verify that there exists a feasible  $\vec{p}$  in the relative interior [24, p. 23] of the domain  $\mathcal{D}$  of the objective function  $-\sum_{\vec{s} \in \mathcal{S}} p_{\vec{s}} \log_e p_{\vec{s}}$ , which is  $\mathcal{D} = \{\vec{p} | p_{\vec{s}} \geq 0 \forall \vec{s} \in \mathcal{S}\}$ . The relative interior of  $\mathcal{D}$  is  $\text{relint } \mathcal{D} = \{\vec{p} | p_{\vec{s}} > 0 \forall \vec{s} \in \mathcal{S}\}$ . Since  $\vec{\theta} \in \mathcal{C}$ , from (12), we can write  $\vec{\theta} = \sum_{\vec{s} \in \mathcal{S}} p_{\vec{s}}^{\bar{\theta}} \vec{s}$ , where  $p_{\vec{s}}^{\bar{\theta}} > 0 \forall \vec{s} \in \mathcal{S}$  and  $\sum_{\vec{s} \in \mathcal{S}} p_{\vec{s}}^{\bar{\theta}} = 1$ . By letting  $\vec{p} = \vec{p}^{\bar{\theta}} \in \text{relint } \mathcal{D}$ , we find a feasible  $\vec{p}$  that satisfies all the constraints in (16). Therefore, Slater's condition is satisfied.

As a result, the optimal solutions to the two convex optimization problems (15) and (16) exist with zero duality gap. Moreover, the dual optimal value is attainable, i.e., there exists a finite  $\vec{r}^*$  such that  $F(\vec{r}^*; \bar{\theta}) = \max_{\vec{r}} F(\vec{r}; \bar{\theta})$ . Therefore, the first-order condition [24, p. 457] of the unconstrained differentiable convex optimization problem in (15) is satisfied at  $\vec{r}^*$ , i.e.,

$$\nabla F(\vec{r}; \bar{\theta}) |_{\vec{r}=\vec{r}^*} = \vec{0} \quad (17)$$

which yields

$$\begin{aligned} \frac{\partial F(\vec{r}; \bar{\theta})}{\partial r_i} |_{\vec{r}=\vec{r}^*} &= \tilde{\theta}_i - \frac{\sum_{\vec{s} \in \mathcal{S}} s_i \exp \left( \sum_{i=1}^N s_i r_i^* \right)}{\sum_{\vec{s} \in \mathcal{S}} \exp \left( \sum_{i=1}^N s_i r_i^* \right)} \\ &= \tilde{\theta}_i - \sum_{\vec{s} \in \mathcal{S}} s_i p_{\vec{s}} = \tilde{\theta}_i - \theta_i^* = 0 \forall i \in \mathcal{N}. \end{aligned} \quad (18)$$

Therefore, for any  $\vec{\theta} \in \mathcal{C}$  (strictly feasible region), the log-likelihood function  $F(\vec{r}; \bar{\theta})$  attains its maximum value at a finite-valued  $\vec{r} = \vec{r}^* \in \mathcal{R}^N$ . At the optimal solution  $\vec{r}^*$ , the first-order optimality condition (17) is satisfied, which corresponds to  $\theta_i^*(\vec{r}^*) = \tilde{\theta}_i \forall i \in \mathcal{N}$ . It is further shown in [25] that  $F(\vec{r}; \bar{\theta})$  is strictly concave in  $\vec{r}$ . Therefore, the optimal solution  $\vec{r}^*$  is unique. ■



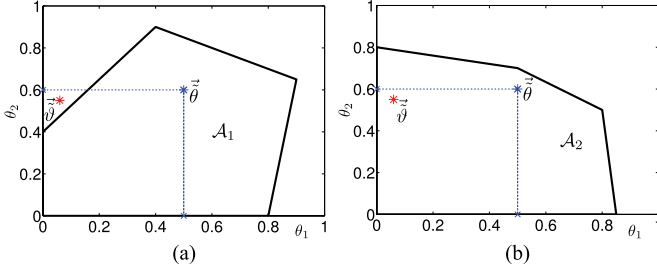


Fig. 5. Examples of 2-D convex “polytopes”. (a) Convex polytope  $\mathcal{A}_1$ , without property in Theorem 1. (b) Convex polytope  $\mathcal{A}_2$ , with property in Theorem 1.

Lemma 1 suggests that, if  $\vec{\theta} \in \mathcal{C}$ , then a unique solution  $\vec{r}^*$  exists such that  $\theta_i^*(\vec{r}^*) = \tilde{\theta}_i \forall i \in \mathcal{N}$ . This proof also suggests that we can solve for  $\vec{r}^*$  by maximizing the concave function  $F(\vec{r}; \vec{\theta})$ . This is useful for the design of our game iteration algorithm presented in Section V-B.

### C. Feasible Throughput Region Under ICN

Previously, we have defined the feasible throughput region for any given set of feasible system states. The shape of the polytopes derived from the ICN model owns a property, which will be discussed here.

We first introduce a binary relation “ $\preceq$ ” between two real-valued vectors  $\vec{\vartheta}$  and  $\vec{\theta}$ , which is defined as component-wise less than or equal to, i.e.,

$$\vec{\vartheta} \preceq \vec{\theta} \Leftrightarrow \vartheta_i \leq \theta_i \forall i \in \mathcal{N}. \quad (19)$$

We now establish the following theorem, which will be useful when presenting our proposed games.

**Theorem 1:** In the ICN model, given that  $\vec{\theta} \in \bar{\mathcal{C}}$  ( $\vec{\theta}$  is in the feasible region), then any desired throughput  $\vec{\vartheta}$ , where  $\vec{0} \preceq \vec{\vartheta} \preceq \vec{\theta}$ , is also in  $\bar{\mathcal{C}}$ .

*Proof:* A first glance at Fig. 4 may lead to the thought that the theorem is trivial, but this is not true. Fig. 5(a) shows a convex set  $\mathcal{A}_1$  in the 2-D space. For a  $\vec{\theta} \in \mathcal{A}_1$ , as shown in Fig. 5(a), it is easy to find a point  $\vec{\vartheta}$  such that  $\vec{\vartheta} \preceq \vec{\theta}$ , and yet  $\vec{\vartheta}$  is not within the convex region  $\mathcal{A}_1$ . On the other hand, it is not difficult to figure out that the convex set  $\mathcal{A}_2$  in Fig. 5(b) owns the property stated in Theorem 1.

In the ICN model, for a target throughput vector  $\vec{\theta}$  where  $\vec{\theta} \in \bar{\mathcal{C}}$ , there exists a probability distribution  $\vec{p}^{\vec{\theta}} = \{p_s^{\vec{\theta}} \forall s \in \mathcal{S}\}$  where  $\vec{\theta} = \sum_{s \in \mathcal{S}} p_s^{\vec{\theta}} \vec{s}$  according to (11). To prove that  $\vec{\vartheta} \preceq \vec{\theta} \in \bar{\mathcal{C}}$ , we need to similarly show that there exists another probability distribution  $\vec{p}^{\vec{\vartheta}} = \{p_s^{\vec{\vartheta}} \forall s \in \mathcal{S}\}$  that fulfills (11). However, it is difficult to obtain the distribution  $\vec{p}^{\vec{\vartheta}}$  directly from  $\vec{p}^{\vec{\theta}}$  since it depends on the underlying link topology.

Our approach is to define an orthotope  $\mathcal{B}$  whose “vertices” are obtained by projecting  $\vec{\theta}$  on all the coordinate planes. An example for the 3-D illustration is shown in Fig. 4. The problem is now becoming equivalent to showing that all the vertices of

$\mathcal{B}$  are in  $\bar{\mathcal{C}}$ . Finally, because  $\vec{\vartheta} \preceq \vec{\theta}$ ,  $\vec{\vartheta}$  is within the cuboid and hence within  $\bar{\mathcal{C}}$ .

We first perform a projection parallel to the  $i$ th axis. Consider a throughput vector  $\vec{\psi}$ , with the setting of  $\psi_i = 0, \psi_j = \tilde{\theta}_j, \forall j \neq i$ , i.e., the  $i$ th link has zero throughput. It is intuitive that  $\vec{\psi}$  is one of the vertices of  $\mathcal{B}$ . To show that  $\vec{\psi}$  is in  $\bar{\mathcal{C}}$ , we need to show that we are able to obtain its state probability distribution  $\{\vec{p}^{\vec{\psi}}\}$  from  $\{\vec{p}^{\vec{\theta}}\}$ , and  $\vec{\psi}$  can be expressed in the form as in (11). This can be done in the following way.

For  $\vec{\theta} \in \bar{\mathcal{C}}$ , its state distribution  $\vec{p}^{\vec{\theta}}$  satisfies  $\vec{\theta} = \sum_{s \in \mathcal{S}} p_s^{\vec{\theta}} \vec{s}$ ,  $p_s^{\vec{\theta}} \geq 0 \forall s \in \mathcal{S}$ , and  $\sum_{s \in \mathcal{S}} p_s^{\vec{\theta}} = 1$ . We next describe how to construct the state distribution  $\vec{p}^{\vec{\psi}}$  for  $\vec{\psi}$ . For those states in  $\mathcal{S}$  with  $s_i = 1$ , choose  $p_s^{\vec{\psi}} = 0$  and  $p_{s-\vec{e}_i}^{\vec{\psi}} = p_{s-\vec{e}_i}^{\vec{\theta}} + p_s^{\vec{\theta}}$ . For the remaining states, choose  $p_s^{\vec{\psi}} = p_s^{\vec{\theta}}$ . In other words, those states  $\vec{s}$  with  $s_i = 1$  should now have state probability  $p_s^{\vec{\psi}} = 0$ . The removed state probability  $p_s^{\vec{\psi}}$  should now be attributed to the state  $\vec{s} - \vec{e}_i$ . It is easy to verify that, by doing so, the total probability remains one, and the throughputs of all unaffected links remain the same as previously. This state probability distribution  $p_s^{\vec{\psi}}$  clearly satisfies (11); hence, the vertex  $\vec{\psi}$  is within  $\bar{\mathcal{C}}$  and so are other vertices of  $\mathcal{B}$ .

For the example shown in Fig. 3, assume that we have a throughput  $\vec{\theta} = [\tilde{\theta}_1, \tilde{\theta}_2, \tilde{\theta}_3] \in \bar{\mathcal{C}}$ . We now show that  $\vec{\psi} = [\tilde{\psi}_1, \tilde{\psi}_2, \tilde{\psi}_3] = [0, \tilde{\theta}_2, \tilde{\theta}_3]$  is also in  $\bar{\mathcal{C}}$ . Note that the throughput  $\vec{\psi}$  is equivalent to the case in which link 1 powers off and stops transmitting. In such a case, there are only three feasible system states left, namely, 000, 010, and 001. In other words, states 100 and 101 disappear and are merged into states 000 and 001, respectively, since link 1 is no longer transmitting. State 010 remains unchanged. Merging the state probability  $p_{101}$  with  $p_{001}$  will ensure that the throughput for link 3 remains the same since  $\tilde{\theta}_3 = p_{001} + p_{101}$ . Merging the state probability  $p_{100}$  with  $p_{000}$  will not affect the throughput of any remaining links. Since the total probability still sum up to one, link 1 will not be transmitting, and both link 2 and link 3 transmit as previously. Therefore, the throughput  $\vec{\psi}$  resulting from these state merging operations is still in  $\bar{\mathcal{C}}$ .

Other vertices of  $\mathcal{B}$  can be also similarly shown to be in  $\bar{\mathcal{C}}$ . Since  $\bar{\mathcal{C}}$  is a convex set and the convex combinations of these vertices are all in  $\bar{\mathcal{C}}$ , we have  $\mathcal{B} \subset \bar{\mathcal{C}}$ . Since  $\vec{\vartheta} \preceq \vec{\theta}$  is enclosed in the hyperrectangle ( $N$ -orthotope),  $\vec{\vartheta}$  should that be in  $\bar{\mathcal{C}}$ . ■

**Remark:** Theorem 1 is not generally true for any convex set. It is true since the values of  $s_i$  are chosen from 0 and 1 only, and the subset of feasible states induced by a maximal independent set is a complete partially ordered set [22] based on how ICN is modeled. For the example in Fig. 3, the maximal independent set  $\{1, 3\}$  induces the subset of three feasible states  $\mathcal{Q} = \{[0, 0, 0], [1, 0, 0], [0, 0, 1], [1, 0, 1]\}$ , which is a complete partially ordered set, with the least element  $[0, 0, 0]$  and the largest element  $[1, 0, 1]$  under the partial order  $\preceq$ . Hence, the use of the theorem needs to be carefully dealt with.

Theorem 1 will be used in Section V-C to show that the pricing problem is a valid quasi-convex optimization problem.

#### D. D2D Network Model

This section discusses how to efficiently model the resulting D2D network if CSMA is adopted by all D2D links. If the objective of the network is to maximize the sum rate of all transmitting links and the BS gives no control on the admission and transmission of links, then, in [11], this problem has been successfully solved. The solution is computed in a completely distributed manner. However, as pointed out previously, such a fully cooperative model is too idealistic, and there is no consideration on the utility heterogeneity and selfish behaviors of the links. It may be better to build a pricing framework so that each link tries to maximize its payoff function when competing for resources, rather than someone trying to take advantage when the network is in operation and drive the network to unstable states. Furthermore, maximizing the sum rate may not distribute the resources according to demand because links with low demand may be assigned to transmit at higher rates due to its spatial location.

In this paper, we feel that the BS can take a more proactive role to assist in D2D transmission. In fact, the problem can be separately formulated in terms of the objectives of the D2D links and the BS. The objective of the BS is to maximize the sum rate while satisfying the physical layer constraints

$$\begin{aligned} \max \quad & \sum_{i=1}^N \tilde{\theta}_i \\ \text{s.t.} \quad & \vec{\theta} \in \mathcal{C} \end{aligned} \quad (20)$$

where  $\tilde{\theta}_i$  is the target rate the network has to support link  $i$ , and the solution must fulfill the CSMA channel access constraint, i.e., the final rates to support all D2D links must be in the strictly feasible throughput region  $\mathcal{C}$  defined in (12).

Each link is a player of a noncooperative game. Each player tries to maximize its payoff  $v_i(\theta_i, \theta_{-i})$  while satisfying the physical layer constraints

$$\begin{aligned} \max \quad & v_i(\theta_i, \theta_{-i}) \quad \forall i \\ \text{s.t.} \quad & \vec{\theta} \in \mathcal{C}. \end{aligned} \quad (21)$$

In (20),  $\tilde{\theta}_i$  is used to represent the rate demand from the utility point of view and should be differentiated from  $\theta_i$  in (9) or (21) used in the ICN model as a result of competing for channel access. At the equilibrium state, these two quantities have to be the same and the pricing mechanism aims to achieve this objective.

There are two challenges in the formulation. These two optimization problems both involve the constraint defined by the strictly feasible throughput region  $\mathcal{C}$ . From Lemma 1 we know that, for any desired throughput  $\vec{\theta}$  in the strictly feasible region  $\mathcal{C}$ , there exists an operating point  $\vec{r}$  such that  $\vec{\theta}(\vec{r}) = \vec{\theta}$ . However, to obtain  $\mathcal{C}$  as in (12), we need to know all the feasible system states, which correspond to all the independent sets [3] in the contention graph. As shown in [3], to compute all the independent sets (including the maximal independent sets) is an NP-hard problem. Hence, it is practically difficult to obtain  $\mathcal{C}$ .

The second challenge is how to align the solution of (20) with the involvement of (21).

Our approach is to develop a simple mechanism that does not require prior knowledge of  $\mathcal{C}$  and yet the radio resource can be allocated to the heterogeneous D2D links efficiently while satisfying the objectives of both the BS and D2D links. A pricing mechanism is introduced to achieve this purpose. The payoff function of each link is made to be dependent on the resource price. The BS broadcasts the resource price and uses it to control the transmission behavior of each link. Mathematically, the BS solves the following optimization problem:

$$\max_{M \geq 0} g(M) := \sum_{i=1}^N \tilde{\theta}_i(M) \quad (22)$$

where  $\tilde{\theta}_i(M)$  is the target rate of D2D link  $i$  under the service price  $M$ , which will be presented in (23). The D2D links are the followers in the overall Stackelberg game, each of which chooses its transmission strategy so that its individual payoff is maximized under the service price chosen by the BS, i.e., the Stackelberg leader.

In the next section, we describe how our proposed Stackelberg game model can achieve this purposes.

#### V. STACKELBERG GAMES FOR NONCOOPERATIVE D2D LINKS

Stackelberg games [12] are a class of noncooperative games in which a leader, who makes the first move in the game, anticipates the actions of the followers based on a model of how the followers would respond to its actions. We propose a Stackelberg game, in which the BS in the cellular network acts as a Stackelberg leader to regulate the transmission behaviors of all the D2D links by broadcasting a proper service price  $M$ . The D2D links are the followers, each of which responds to the price  $M$  by choosing its transmission strategy in an attempt to maximize its individual payoff.

In Section V-A, we first define the utility functions for the D2D links, each of which characterizes the individual service requirements and willingness to pay. In Section V-B, we study the noncooperative behaviors of the D2D links under a given network price  $M$ , which defines the follower subgame in the Stackelberg game. The Stackelberg game is analyzed in Section V-C. Based on the analysis, the pricing strategies of the Stackelberg leader are proposed in Section V-D. A brief complexity analysis is given in Section V-E.

##### A. D2D Link Utility Function

We modify the traffic model used in [27] to our system. Suppose that D2D link  $i$  has a target rate  $\theta_i$  in the range of  $[\gamma_i, \pi_i]$ , where  $\gamma_i \leq \theta_i \leq \pi_i$ . If  $\theta_i < \gamma_i$ , link  $i$  achieves zero utility, and each link has no intention to go beyond  $\theta_i > \pi_i$ . The exact target rate value  $\theta_i$  is controlled by the service price  $M$  through the following relationship:

$$\tilde{\theta}_i(M) = \begin{cases} 0, & M > m_i \\ \min \{ \gamma_i - b_i(M - m_i), \pi_i \}, & 0 \leq M \leq m_i \end{cases} \quad (23)$$

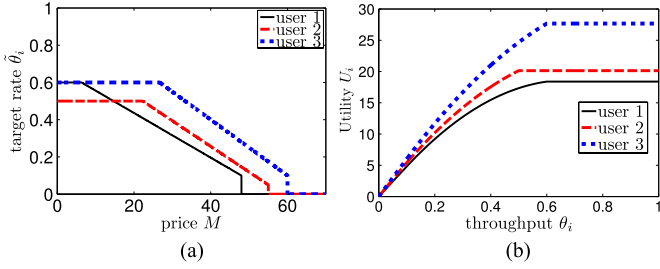


Fig. 6. Target rates and utility functions of the CSMA users. (a) Target rates of the CSMA users under the price  $M$ . (b) Utility functions of the three CSMA users.

where  $\gamma_i$ ,  $\pi_i$ , and  $m_i$  together decide how link  $i$  is willing to pay for the transmission. For simplicity, we have adopted a monotonically decreasing linear function for  $\tilde{\theta}_i(M)$  in the range  $\gamma_i \leq \tilde{\theta}_i \leq \pi_i$ , where  $b_i$  is a positive coefficient and  $-b_i$  is the slope.

Equation (23) is interpreted as follows. Parameter  $m_i$  is the highest price that link  $i$  is willing to pay for its transmission. When  $M = m_i$ , link  $i$  will only desire a minimum throughput of  $\gamma_i$ . When the price is too high (i.e.,  $M > m_i$ ), link  $i$  chooses not to transmit, and thus, its target rate drops to zero, i.e.,  $\tilde{\theta}_i(M) = 0$ . Over the range  $0 \leq M \leq m_i$ , link  $i$  is willing to pay for its transmission, and the lower the price  $M$ , the higher throughput it desires, unless it has already reached its maximum desired throughput  $\pi_i$ . In this range, we have used a linear function to simplify this monotonic relationship. Other function forms such as hyperbolic, parabolic, and cubic can be also used as long as the monotonic relationship is preserved. As a result, the relationship in (23) is a piecewise linear function. In the special case in which the minimum desired throughput is  $\gamma_i = 0$  and the maximum desired throughput is  $\pi_i \geq b_i m_i$ , the piecewise linear relationship in (23) simply reduces to a smooth linear relationship. A smooth monotonic curve can be similarly obtained when other function forms are adopted. Note that our algorithm works if only the monotonic function property holds.

The utility function is designed to provide differentiated treatment for the links based on their actual demand and willingness to pay for the desired transmission rate. For the example given in Fig. 6(a), D2D link 1 and link 3 have the same range in their target rates, i.e.,  $\pi_1 = \pi_3$  and  $\gamma_1 = \gamma_3$ , and link 3 has a higher willingness to pay, i.e.,  $m_3 > m_1$ . When the price  $M$  continually decreases from a large value until zero, link 3 will be admitted into the system first.

From the game-theoretic perspective, link  $i$  will try to choose its target rate  $\tilde{\theta}_i$  to maximize its own payoff  $v_i(\theta_i) = U_i(\theta_i) - M\theta_i$  (utility minus cost). To be compatible with such an incentive, we can reversely derive the utility function of D2D link  $i$  as follows. If the utility function  $U_i(\theta_i)$  is concave, then the  $\theta_i$  value that maximizes  $v_i(\theta_i)$  is given by the first-order condition  $v'_i(\theta_i) = 0$ , i.e.,  $\tilde{\theta}_i = (U'_i)^{-1}(M)$ . Equating with the example of (23), we can reversely derive the utility function for D2D link  $i$

$$U_i(\theta_i) = \begin{cases} m_i\theta_i, & 0 \leq \theta_i < \gamma_i \\ m_i\theta_i - \frac{(\theta_i - \gamma_i)^2}{2b_i}, & \gamma_i \leq \theta_i < \pi_i \\ m_i\pi_i - \frac{(\pi_i - \gamma_i)^2}{2b_i}, & \pi_i \leq \theta_i \leq 1. \end{cases} \quad (24)$$

The utility functions for the three links' example in Fig. 6(a) are plotted in Fig. 6(b). If we take the derivative of  $U_i(\theta_i)$  on  $\theta_i$  in (24), it can be seen that a higher  $m_i$  value corresponds to a steeper slope, which suggests a higher willingness to pay. This is shown in Fig. 6(b), in which the utility function of link 3 has a steeper slope than the utility function of link 1.

### B. Subgame of Noncooperative CSMA Users

The Stackelberg game at the  $l$ th stage begins with the BS broadcasting a price  $M^{(l)}$ . Each D2D link  $i$  ( $i \in \mathcal{N}$ ) aims to maximize its payoff  $v_i(\theta_i) = U_i(\theta_i) - M^{(l)}\theta_i$ . According to the analysis in Section V-A, link  $i$ 's objective is equivalent to attaining a target rate  $\tilde{\theta}_i^{(l)}$  under the service price  $M^{(l)}$ , as given in (23). Whether these target rates are achievable still depends on whether the underlying CSMA mechanism can support these transmissions. The D2D links therefore play a CSMA game among themselves to determine their individual TAs to make the throughput  $\theta_i$  as close to  $\tilde{\theta}_i^{(l)}$  as possible. This CSMA game is therefore the follower subgame in the Stackelberg game. To avoid the links from transmitting too aggressively and driving the network to unstable states as a result of congestion, a simple approach is to let  $M$  begin with a large value and then gradually decrease that value.

We formally state the CSMA subgame as follows.

**Players:** Distributed Tx–Rx pairs (D2D links),  $i \in \mathcal{N}$ , who compete to transmit in the ICN.

**Strategies:** Each player  $i$  chooses its TA  $r_i \in \mathcal{R} \forall i \in \mathcal{N}$ .

**Objectives:** Each player  $i$  ( $i \in \mathcal{N}$ ) aims to achieve its target rate  $\tilde{\theta}_i^{(l)}$  set by maximizing its payoff

$$v_i(\theta_i) = U_i(\theta_i) - M^{(l)}\theta_i \quad (25)$$

under the given service price  $M^{(l)}$ .

Note that the throughput  $\theta_i$  that player  $i$  can achieve is determined by its own TA  $r_i$  and the TAs of all the other players  $r_{-i}$ , based on the relationships in (9). The equilibrium solution of the CSMA subgame is a *Nash equilibrium (NE)* [12], which is defined as a strategy profile  $\vec{r}^* = [r_1^*, \dots, r_N^*]$  in which player  $i$ 's strategy  $r_i^*$  is a best response to the strategies  $r_{-i}^*$  of all the other players, i.e.,

$$r_i^* = \arg \min_{r_i \in (-\infty, +\infty)} \left| \tilde{\theta}_i^{(l)} - \theta_i(r_i, r_{-i}^*) \right| \quad \forall i \in \mathcal{N} \quad (26)$$

where  $\theta_i(\vec{r})$  is the achieved throughput of D2D link  $i$  in the ICN model, as given in (9).

It is clear that the objective of the subgame is to find the equilibrium TAs for all D2D links so that every link achieves throughputs that are as close to what are desired. According to Lemma 1, if the target rate  $\tilde{\theta}$  is in  $\mathcal{C}$ , i.e., it is achievable, then there exists a unique TA  $\vec{r}^*$  such that  $\theta_i^*(\vec{r}^*) = \tilde{\theta}_i^{(l)} \forall i \in \mathcal{N}$ .

On the other hand, if the target rate  $\tilde{\theta}$  is beyond  $\mathcal{C}$ , during the myopic best response updates, all players will keep increasing their TAs if their throughputs are lower than their respective



target rates, i.e., all links transmit aggressively and result in undesired network congestion. The existence and uniqueness of the NE in the CSMA subgame can be then established in the following proposition.

**Proposition 1:** For the target rate  $\vec{\theta} \in \mathcal{C}$  (strictly feasible region), there exists a unique finite-valued NE  $\vec{r}^* \in \mathcal{R}^N$  in the CSMA subgame. Moreover, the target rate  $\vec{\theta}$  is achieved at the NE, i.e.,  $\vec{\theta}^*(\vec{r}^*) = \vec{\theta}$ .

**Proof:** From Lemma 1, if the target rate  $\vec{\theta} \in \mathcal{C}$  (strictly feasible region), then there exists a unique finite-valued  $\vec{r}^* \in \mathcal{R}^N$  such that  $\vec{\theta}^*(\vec{r}^*) = \vec{\theta}$ . As shown in (26), there exists a unique NE  $\vec{r}^*$  since the payoff of each player is maximized when  $\vec{\theta}^*(\vec{r}^*) = \vec{\theta}$ , and no player has the incentive to deviate from this NE unilaterally. ■

In practice, the strategies of all the other players  $r_{-i}$  are usually not known by player  $i$  if we assume that there is no explicit information exchange among the players. We therefore design some distributed updating method for the players to arrive at the NE. Let each player update its strategy by measuring its own local statistics, e.g., measured throughput  $\hat{\theta}_i$ . For the  $k$ th measurement period  $\tau(k)$ , player  $i$  keeps a record of the accumulated transmission time  $T_i(k)$  and obtains the empirical average throughput as

$$\hat{\theta}_i(k) = T_i(k)/\tau(k) \quad \forall i \in \mathcal{N}. \quad (27)$$

A distributed way for player  $i$  to update its strategy can be

$$r_i(k+1) = r_i(k) + \alpha \cdot (\tilde{\theta}_i^{(l)} - \hat{\theta}_i(k)) \quad \forall i \in \mathcal{N} \quad (28)$$

where  $\alpha$  is a small positive step size. The conditions for the convergence of the NE in the CSMA subgame are summarized in the following proposition.

**Proposition 2:** For the target rate  $\vec{\theta} \in \mathcal{C}$  (strictly feasible region), the iteration dynamics in (28) with a small-enough step size  $\alpha$  and a long-enough measurement period  $\tau$  will always converge to the NE  $\vec{r}^* \in \mathcal{R}^N$  in the CSMA subgame.

**Proof:** We apply the same idea used when proving Lemma 1. Given a  $\vec{\theta} \in \mathcal{C}$ , we use the maximum log-likelihood method to estimate the parameters  $\vec{r}^*$  that result in  $\vec{\theta}(\vec{r}^*) = \vec{\theta}$  or, equivalently, result in the desired state probability distribution  $\vec{p}^{\vec{\theta}}$  such that  $\vec{\theta}(\vec{r}^*) = \sum_{\vec{s} \in \mathcal{S}} p_{\vec{s}}^{\vec{\theta}} \vec{s}$ . The log-likelihood function  $F(\vec{r}; \vec{\theta})$  is given in (14). It was shown in Section IV-B that  $F(\vec{r}; \vec{\theta})$  is a strictly concave function in  $\vec{r}$  and attains its maximum when  $\vec{\theta}(\vec{r}^*) = \vec{\theta}$ . Therefore, we can use the subgradient method [28] to obtain the optimal solution  $\vec{r}^*$ , where  $\tilde{\theta}_i^{(l)} - \hat{\theta}_i(k)$  is an estimation of the gradient  $\partial F(\vec{r}; \vec{\theta}) / \partial r_i$  [see (18)] in the  $k$ th measurement period. Since the objective function  $F(\vec{r}; \vec{\theta})$  is differentiable and concave in  $\vec{r}$ , the subgradient method with constant step size  $\alpha$  yields convergence to the optimal value, provided that the step size  $\alpha$  is small enough and the measurement period is long enough [28]. In summary, this proposition follows. ■

As aforementioned, under the myopic best response update approach, if the target rate  $\vec{\theta}$  is beyond  $\mathcal{C}$ , all players will keep increasing their TAs if their throughputs are lower than their respective target rates, and the network will be pushed into an undesired congested situation. To overcome this problem, we impose an upper limit  $r_{\max}$  on  $r_i \forall i \in \mathcal{N}$  as an implementation constraint. The iteration dynamics in (28) then become

$$r_i(k+1) = \min \left\{ r_i(k) + \alpha \cdot (\tilde{\theta}_i^{(l)} - \hat{\theta}_i(k)), r_{\max} \right\} \quad \forall i \in \mathcal{N}. \quad (29)$$

The physical meaning of imposing the  $r_{\max}$  constraint is to refrain the D2D links from transmitting too aggressively so that the local congestion at some links will not affect the whole network. The outcome of introducing such a restriction is that the feasible throughput region will shrink into a subset of the original one. Hence, the solution obtained with this constraint imposed is always ensured to be within  $\mathcal{C}$ . During the myopic play, if any link arrives at  $r_{\max}$ , the BS will be informed. Then, the price  $M$  is frozen and the whole D2D network functions at the boundary of the “shrunk” feasible throughput region. If this happens, not all users are able to achieve their desired rates or even admitted as the network is in congestion.

### C. Analysis of the Stackelberg Game

Here, we analyze the structure of the Stackelberg game. From Proposition 1 and Proposition 2, to satisfy  $\vec{\theta} \in \mathcal{C}$ , it is equivalent to checking that the CSMA subgame converges to the unique subgame NE  $\vec{r}^*$  defined in (26) under the given service price  $M$ . Therefore, the leader problem in (22) is equivalent to the following optimization problem:

$$\begin{aligned} & \max_{M \geq 0} g(M) \\ & \text{s.t.} \begin{cases} \text{equality constraint (23)} \quad \forall i \in \mathcal{N} \\ \text{equality constraint (26)} \\ r_i^* < r_{\max} \quad \forall i \in \mathcal{N} \end{cases} \end{aligned} \quad (30)$$

where  $r_i^*$  is the TA of D2D link  $i$  at the NE of the CSMA subgame, as given in (26). The constraint  $r_i^* < r_{\max} \quad \forall i \in \mathcal{N}$  implies that the target rate  $\vec{\theta}$  as given in (23) is strictly feasible at the subgame NE, i.e., the throughput will converge to  $\vec{\theta}^*(\vec{r}^*) = \vec{\theta}$  in the CSMA subgame.

To distinguish from the NE  $\vec{r}^*$  in the CSMA subgame, we call the equilibrium solution  $(M^{\text{opt}}, \vec{r}^{\text{opt}})$  of the Stackelberg game as the Stackelberg equilibrium [29], where  $M^{\text{opt}}$  is the optimal solution to (30) and  $\vec{r}^{\text{opt}}$  is the subgame NE under the price  $M^{\text{opt}}$ .

The problem in (30) is nonconvex [24, p. 136] since the objective function  $g(M) = \sum_{i=1}^N \hat{\theta}_i(M)$  is nonconcave in  $M$  and the equality constraints (23) and (26) are nonlinear. Fortunately, the problem can be converted into a quasi-convex optimization problem [24, p. 144], and the solution can be iteratively evaluated by solving a sequence of convex optimization problems. It can be interpreted in the following way. Since the target rate  $\hat{\theta}_i(M)$  of each D2D link  $i$  is nonincreasing with the price  $M$ ,

the chain of prices  $M^{(0)} > M^{(1)} > \dots > M^{(l)} > M^{(l+1)}$  induces a chain of target rates  $\vec{\theta}^{(0)} \succeq \vec{\theta}^{(1)} \succeq \dots \succeq \vec{\theta}^{(l)} \succeq \vec{\theta}^{(l+1)}$ . Therefore, the objective function  $g(M) = \sum_{i=1}^N \bar{\theta}_i(M)$  is also nonincreasing with  $M$  and hence is quasi-concave in  $M$ . Regarding the constraints in (30), from Lemma 1, if the target rate  $\vec{\theta}^{(l)} \in \mathcal{C}$  (strictly feasible throughput region, which is the interior of the feasible throughput region  $\bar{\mathcal{C}}$ ), then it is achievable with finite-valued TAs  $\vec{r}^*$ . On the other hand, from Theorem 1, if the target rate  $\vec{\theta}^{(l)} \notin \bar{\mathcal{C}}$ , then any target rate  $\vec{\theta}^{(l+1)} \succeq \vec{\theta}^{(l)}$  is not in  $\bar{\mathcal{C}}$ , i.e., it is not achievable, and the constraints in (30) are not satisfied. The crossing from within  $\bar{\mathcal{C}}$  to beyond can be detected by the use of  $r_{\max}$ . Therefore, the superlevel set  $\{M | g(M) \geq G\}$  is convex, which is equivalent to the line segment  $\{M | g^{-1}(\sup g) \leq M \leq g^{-1}(G)\}$ , where  $G$  is a constant,  $g^{-1}$  is the inverse function of  $g(M)$ , and  $\sup g$  is the optimal value of (30).

In summary, the problem in (30) is quasi-convex [24, pp. 137 and 144] since the objective function  $g(M)$  to be maximized is quasi-concave, and the superlevel set  $\{M | g(M) \geq G\}$  is convex. As a result, the problem in (30) can be reduced into a sequence of feasibility problems

$$\begin{aligned} \text{find } & M \\ \text{s.t. } & \begin{cases} g(M) \geq G \\ \text{equality constraint (23)} \forall i \in \mathcal{N} \\ \text{equality constraint (26)} \\ r_i^* < r_{\max} \forall i \in \mathcal{N}. \end{cases} \end{aligned} \quad (31)$$

If problem (31) is feasible, then the maximum total throughput  $\sup g$  is not less than  $G$ . Conversely, if problem (31) is infeasible, then we can conclude that  $\sup g < G$ . To find the optimal value  $\sup g$  to problem (30), we can test different superlevels  $G$  in feasibility problem (31).

For each superlevel  $G$ , from the proof of Proposition 2, the feasibility problem in (31) is equivalent to the following max-log-likelihood problem:

$$\begin{aligned} \max_{\vec{r}} & F(\vec{r}; \vec{\theta}) \\ \text{s.t. } & \begin{cases} \text{equality constraint (23)} \forall i \in \mathcal{N} \\ M = g^{-1}(G) \\ r_i < r_{\max} \forall i \in \mathcal{N} \end{cases} \end{aligned} \quad (32)$$

where  $F(\vec{r}; \vec{\theta})$  is the log-likelihood function defined in (14). In other words, if problem (31) is feasible, then there exists a price  $M = g^{-1}(G)$ , such that the target rate  $\vec{\theta}(M)$  is achievable with finite TA  $r_i < r_{\max} \forall i \in \mathcal{N}$ . Therefore, we can use the max-log-likelihood method to estimate the parameters  $\vec{r}$  that achieve the target rate  $\vec{\theta}(M)|_{M=g^{-1}(G)}$ , as given in (23). Notice that, given constant  $G$ , the price  $M$  and the target rate  $\vec{\theta}$  become constant values as well. Moreover, as shown in the proof of Proposition 2, the log-likelihood function is concave in  $\vec{r}$ . As a result, the max-log-likelihood problem in (32) is a convex optimization problem and can be solved by the subgradient updating method in (29).

If the iteration dynamics converge to a subgame NE with  $r_i^* < r_{\max} \forall i \in \mathcal{N}$ , then the optimal solution to (32) exists, i.e., problem (31) is feasible. Otherwise, if the iteration dynamics in (29) converge to a subgame NE with  $r_i^* = r_{\max}$  and  $\bar{\theta}_i^* < \bar{\theta}_i$  for some D2D link  $i$ , then the optimal solution to (32) does not exist, and problem (31) is infeasible, i.e., not all D2D links' target rates are being achieved.

In summary, the problem in (30) can be reduced into a sequence of convex optimization problems. A simple bisection method can be used to choose the superlevels  $G$  [or, equivalently, the price  $M = g^{-1}(G)$ ] and test the feasibility problem (31). Alternatively, we can borrow ideas from the feasible direction method [30, Ch. 10], which avoids testing in the infeasible region, and design the pricing strategies to keep the network operating in the feasible region while tuning the price  $M$ .

#### D. Pricing Strategies of the Stackelberg Leader

We call each round of CSMA subgame under a certain price  $M$  as a *stage* in the Stackelberg game. In each stage, the leader needs the feedback from each D2D link  $i$  about its target rate  $\bar{\theta}_i$  and the converged TA  $r_i^*$  and throughput  $\bar{\theta}_i^*$ . Notice that the leader only has knowledge about the monotonicity of the D2D link's target rate with the price  $M$ , and no information about (23) of all links is required.

Under some low-load situations, all links achieve their maximum desired throughput  $\pi_i \forall i \in \mathcal{N}$ , if for all links  $i \in \mathcal{N}$ , the target rate  $\bar{\theta}_i > 0$  and remains unchanged between two consecutive prices  $M^{(l)}$  and  $M^{(l+1)}$ . Under heavy-load situations, the pricing strategies of the Stackelberg leader need to be carefully designed to converge to the optimal price  $M^{\text{opt}}$ .

To detect convergence, we define  $\Delta_i = r_{\max} - r_i^*$  as the "margin" of TA for each D2D link  $i \in \mathcal{N}$ . When the achieved target rates are close to the capacity boundary, the leader can make use of  $\Delta_{\min} = \min\{\Delta_i \forall i \in \mathcal{N}\}$  as an indication of how close the current throughput  $\bar{\theta}^*$  is to the boundary of  $\mathcal{C}$ . Since the total throughput  $g(M)$  is nonincreasing with the price  $M$ , the leader can gradually decrease  $M$  to increase  $g(M)$  until the constraint  $r_i^* < r_{\max}$  is critically satisfied for some D2D link says  $i$ , i.e.,  $\Delta_{\min} \leq \epsilon$ , where  $\epsilon$  is a small positive threshold.

The algorithm at the BS works as follows. In the 0th stage, the leader can start with a large price  $M^{(0)}$  so that the network starts with a low load. Similar to the Newton method [24, p. 488], which applies line search to narrow the searching region before using Newtonian steps to refine the optimal solution, the adjustment of our price strategies consists of two phases as well. In the first phase, the leader uses a relatively large decrement step  $\phi$  to decrease price  $M$  until  $\Delta_{\min} \leq \eta$ , where  $\eta > \epsilon$  is a threshold before entering the second phase. In the second phase, the decrement steps are refined using  $\Delta_{\min}$  since  $\Delta_{\min}$  is getting smaller as the target rates are approaching the boundary of the feasible throughput region.

In summary, the leader can update its price  $M$  based on  $\Delta_{\min}$  at the end of the  $l$ th stage as follows:

$$M^{(l+1)} = \begin{cases} M^{(l)} - \phi, & \Delta_{\min} > \eta \\ \max\{M^{(l)} - \beta \cdot \Delta_{\min}, M_{\text{lower}}\}, & \Delta_{\min} \leq \eta \end{cases} \quad (33)$$

where  $\phi$  is a positive constant, and  $\beta$  is a positive parameter.  $M_{\text{lower}}$  is initially set at 0 and is updated to take the value of current  $M^{(l)}$ , once it is detected that the solution for the target rate  $\vec{\theta}$  is outside the feasible region. Its purpose is to ensure that subsequent  $M^{(l+1)}, \dots$ , should not go below this value. Parameter  $\beta$  can be chosen to be small enough so that the price gradually decreases until  $\Delta_{\min} \leq \epsilon$ . However, for faster convergence, it might happen that the initially chosen  $\beta$  is too large so that the new price  $M^{(l+1)}$  pushes the target rate  $\vec{\theta}$  outside the feasible region, i.e.,  $r_i^* = r_{\max}$  but  $\theta_i^* < \tilde{\theta}_i$  for some D2D link  $i$ . In such cases, the leader stores the current unachievable price as the new lower bound  $M_{\text{lower}}$ , resets the price to the previously found achievable price  $M_{\text{prev}}$ , and reduces  $\beta$  by a discount factor  $\sigma$ , e.g.,  $\sigma = 0.9$ .

The pricing strategies of the leader and the CSMA subgame are summarized in Algorithm 1. Through Algorithm 1, the Stackelberg game is guaranteed to gradually converge to the optimal price  $M^{\text{opt}}$  under which the total throughput of the CSMA users is maximized, while their heterogeneous target rates can all be satisfied.

---

**Algorithm 1** Iteration Process of the Stackelberg Game

---

```

1: Initialize:
2: The BS chooses the initial price  $M = M^{(0)}$  and informs
   the D2D links in the control plane;
3: Each D2D link  $i \in \mathcal{N}$  chooses the initial TA  $r_i(0)$ ;
4: repeat:
5:   In the  $l$ th stage:
6:   for  $i = 1, \dots, N$  D2D links do:
7:     Set target rate  $\tilde{\theta}_i^{(l)}$  based on price  $M^{(l)}$ , as in (23);
8:   end for
9:
10:  repeat:
11:    In the  $k$ th measurement period:
12:    for  $i = 1, \dots, N$  users do:
13:      Estimate the empirical throughput  $\hat{\theta}_i(k)$ , as in (27);
14:      Update the TA  $r_i(k+1)$ , as in (29);
15:    end for
16:     $k \leftarrow k + 1$ ;
17:  until  $\vec{r}$  converges to the subgame NE  $\vec{r}^*$ .
18:  Each user  $i \in \mathcal{N}$  informs the BS about  $\tilde{\theta}_i^{(l)}$ ,  $r_i^*$  and  $\theta_i^*$ ;
19:
20:  At the BS:
21:   $\Delta_{\min} = \min_{i \in \mathcal{N}} \Delta_i = \min_{i \in \mathcal{N}} (r_{\max} - r_i^*)$ ;
22:  if  $\Delta_{\min} > \epsilon$  then:
23:    set  $M^{(l+1)}$  as in (33);  $M_{\text{prev}} = M^{(l)}$ ;  $\Delta_{\text{prev}} = \Delta_{\min}$ .
24:  else if  $0 < \Delta_{\min} \leq \epsilon$  or  $(\vec{\theta}^{(l)} \succ \vec{0} \text{ and } \vec{\theta}^{(l)} = \vec{\theta}^{(l-1)})$  then:
25:    The Stackelberg game converges with  $M^{\text{opt}} = M^{(l)}$ ;
    go to END.
26:  else if  $r_i^* = r_{\max}$  but  $\theta_i^* < \tilde{\theta}_i$  for some user  $i$  then:
27:     $M_{\text{lower}} = M^{(l)}$ ;  $\beta \leftarrow \sigma \cdot \beta$ ;  $M^{(l+1)} = \max\{M_{\text{prev}} - \beta \cdot \Delta_{\text{prev}}, M_{\text{lower}}\}$ .
28:  end if
29:   $l \leftarrow l + 1$ ;
30: until The Stackelberg game converges. END.

```

---

An important side information that can be provided by the proposed algorithm is the identification of the bottleneck link in the heterogeneous D2D networks. Upon convergence of the Stackelberg game, the D2D link  $L = \arg \min \{\Delta_i \mid i \in \mathcal{N}\} = \arg \min \{r_{\max} - r_i^{\text{opt}} \mid i \in \mathcal{N}\}$  is the bottleneck link to the network since any further decrease in the price  $M^{\text{opt}}$  would drive the target rate  $\vec{\theta}$  outside the capacity region, and link  $L$  can no longer achieve its target rate. The identification of such bottleneck links can be of valuable information, for example, in data offloading, to reassign these links back to the cellular network when necessary. How to achieve optimal trade-off remains as interesting future work.

### E. Complexity of Algorithm 1

Algorithm 1 consists of two loops. In the outer loop, the BS chooses a service price  $M^{(l)}$  at the  $l$ th stage according to the pricing strategies in Section V-D. In the inner loop, for each given service price  $M^{(l)}$ , the D2D links play the CSMA subgame distributively and iteratively until converging to their respective target rates. We analyze the complexity in terms of the number of iterations required, first for the CSMA subgame, then for the pricing strategies.

For the CSMA subgame, assume that the target rate  $\vec{\theta}$  under the given service price  $M^{(l)}$  is in the strictly feasible region  $\mathcal{C}$ . According to Proposition 1 and Proposition 2, the distributed strategy updates of the CSMA users in (28) are equivalent to the gradient method in maximizing the log-likelihood function  $F(\vec{r}; \vec{\theta})$ , which is differentiable and strictly concave in  $\vec{r}$ . In particular, the gradient of  $F(\vec{r}; \vec{\theta})$  is  $\nabla F(\vec{r}; \vec{\theta}) = \vec{\theta} - \vec{\theta}(\vec{r})$ , as shown in (18). Since the maximum value of  $F(\vec{r}; \vec{\theta})$  is finite and attained at  $\vec{r}^*$ , this means that  $\vec{\theta}^*(\vec{r}^*) = \vec{\theta}$  can be solved by setting the gradient  $\nabla F(\vec{r}^*; \vec{\theta}) = \vec{0}$ .

Since the norms of the throughput  $\vec{\theta}(\vec{r})$  and its gradient  $\nabla \vec{\theta}(\vec{r})$  are both bounded, it can be shown that  $\nabla F(\vec{r}; \vec{\theta})$  is Lipschitz continuous [31] in  $\vec{r}$ , i.e.,  $\|\nabla F(\vec{r}_a; \vec{\theta}) - \nabla F(\vec{r}_b; \vec{\theta})\| = \|\vec{\theta}(\vec{r}_a) - \vec{\theta}(\vec{r}_b)\| \leq H \|\vec{r}_a - \vec{r}_b\| \forall \vec{r}_a, \vec{r}_b \in \mathcal{R}^N$ , where  $H$  is a positive constant. According to Theorem 1 in [31, Sec. 1.4] and Theorem 2.1.14 in [32, Sec. 2.1.5], for a small-enough step size  $\alpha$  ( $0 < \alpha \leq 1/H$ ), the number of iterations to reach  $\|\nabla F(\vec{r}; \vec{\theta})\| = \|\vec{\theta} - \vec{\theta}(\vec{r})\| < \xi$  is  $O(1/\xi)$  (i.e., no more than a fixed multiple of  $1/\xi$ ).

It is worth to mention that, although this complexity  $O(1/\xi)$  on the number of required iterations is independent on the number of users, we have inherently assumed that the measurement period  $\tau$  is long enough to provide an accurate estimation of throughputs. In fact, the choice of  $\tau$  depends on the number of users and the underlying topology. The purpose of choosing a large  $\tau$  is to ensure that the Markov chain corresponding to the updated  $\vec{r}$  reaches its stationary distribution to allow for an accurate estimation of throughputs. In general, a larger number of users requires a larger value of  $\tau$ . More comparisons and discussions on how to choose  $\tau$  for a given number of users and different topologies can be found in [25].

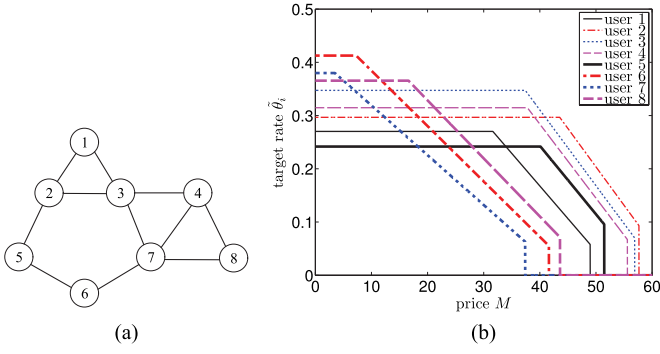


Fig. 7. Topology and target rates of eight D2D links. (a) Contention graph. (b) Target rates under price  $M$ .

We now briefly discuss how to estimate the number of pricing stages required in the outer loop. This analysis is complicated by the fact that the step sizes for  $M$  are changing each time. Assume that the maximum value of the price is  $M_{\max}$ . In phase 1 of the price setting, since the price is decreasing at a large constant step  $\phi$ , the number of pricing stages in phase 1 is capped by  $\lceil M_{\max}/\phi \rceil$  or  $\lceil M_{\max}/\phi \rceil/2$  on average. In phase 2, the TA margin  $\Delta_{\min} \leq \eta$ , and the price is already close to the optimal. In the algorithm, we refine the price change  $\delta M^{(l+1)} = M^{(l+1)} - M^{(l)}$  at stage  $l$  according to  $\delta M^{(l+1)} = -\beta \Delta_{\min}^{(l)}$  progressively until the TA margin gradually approaches the required precision  $\epsilon$ , i.e.,  $\Delta_{\min} \leq \epsilon$ . Assuming that the interval  $\epsilon < \Delta_{\min} \leq \eta$  is small, through simulations, we find that the relationship between the TA margin  $\Delta_{\min}^{(l+1)}$  and the price change  $\delta M^{(l+1)}$  can be approximated by  $\Delta_{\min}^{(l+1)} = \Delta_{\min}^{(l)} + B \cdot \delta M^{(l+1)}$ , where  $B$  is a positive constant. Since we set  $\delta M^{(l+1)} = -\beta \Delta_{\min}^{(l)}$ , hence  $\Delta_{\min}^{(l+1)} = \Delta_{\min}^{(l)} + B \cdot (-\beta \Delta_{\min}^{(l)}) = (1 - \beta B) \Delta_{\min}^{(l)}$ . The TA margin then follows a geometric progression, and we can estimate the value of  $h$  so that  $\delta M^{(l+h)} \leq \epsilon$ . Hence, it can be easily shown that the number of stages for  $\Delta_{\min}$  to decrease from  $\eta$  to  $\epsilon$  is approximately  $(\log_{10} \eta/\epsilon)/(\log_{10} 1/(1 - \beta B))$  or  $O(d \log_{10}(\eta/\epsilon))$  for some suitable choices of  $\beta$  and  $B$  ( $0 < \beta B < 1$ ), where  $d = 1/(\log_{10} 1/(1 - \beta B))$ . Note that  $\beta$  can be chosen according to the value of  $B$ , but  $B$  is topology and utility dependent. As a result, the total number of stages required for convergence is  $O(1/\phi) + O(d \log_{10}(\eta/\epsilon))$ .

In summary, the number of iterations required for convergence in the proposed game is given by the number of iterations per stage multiplied by the required number of stages, i.e.,  $O(1/\xi) \cdot (O(1/\phi) + O(d \log_{10}(\eta/\epsilon)))$ .

## VI. SIMULATION STUDY

Here, we demonstrate the Stackelberg game via an example. Consider the eight D2D links' contention graph in Fig. 7(a). Assume that the relationships between the links' target rates and the price  $M$  are given as in Fig. 7(b). In the ICN model, we assume that the links' transmission time is uniformly distributed with mean of 1 ms in the range of [0.5, 1.5] ms. Further assume that link  $i$ 's backoff time is uniformly distributed with mean of  $1/\exp(r_i)$  ms in the range  $[0, 2/\exp(r_i)]$  ms.

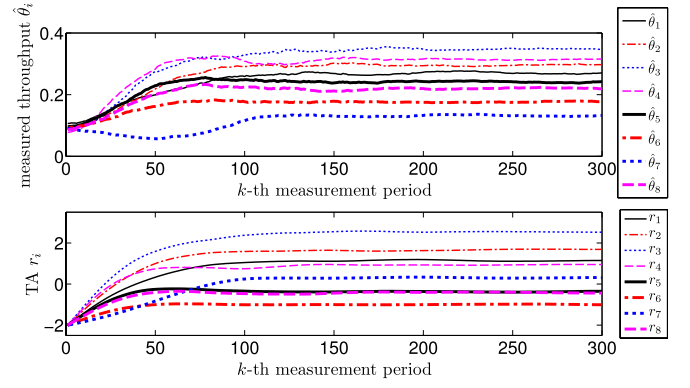


Fig. 8. CSMA subgame of the eight D2D links under  $M = 30$ .

### A. CSMA Subgame

Assume that the current price  $M = 30$ , and then from Fig. 7(b), we know that the D2D links' target rates are  $\vec{\theta} = [0.270, 0.297, 0.347, 0.315, 0.242, 0.176, 0.132, 0.220]$ . Assume that the initial TAs  $r_i = -2 \forall i \in \mathcal{N}$ . The CSMA subgame is then played according to lines 10–17 in Algorithm 1. In the  $k$ th measurement period, we apply a simple averaging filter to smooth the measured throughput as

$$\hat{\theta}_i(k) = (1 - \delta) \cdot \hat{\theta}_i(k-1) + \delta \cdot T_i(k)/\tau \quad \forall i \in \mathcal{N} \quad (34)$$

where  $\delta$  is the weight of the new measurement. In our simulations, we choose  $\delta = 0.05$ , and the measurement time  $\tau = 200$  ms. A smaller value of  $\delta$  not only makes the measured throughput more smooth but also increases the convergence time. To update TAs as in (29), we choose the step size  $\alpha = 0.4$ , and the maximum allowable TA  $r_{\max} = 3$ . Note that a smaller value of  $\alpha$  not only guarantees the convergence of the CSMA subgame but also increases the convergence time. The iteration process of the CSMA subgame is then plotted in Fig. 8. The CSMA subgame converges to 99% of the target rates ( $\xi = 1\%$ ) in around 150 iterations. According to the complexity analysis in Section V-E, the number of required iterations is  $O(1/\xi)$ , i.e., on the order of a fixed multiple of  $1/\xi = 100$ . Thus, our simulation result is on the same order as the previous prediction.

### B. Stackelberg Game

Assume that the initial price  $M^{(0)} = 55$ ,  $\phi = 5$ ,  $\beta = 5$ ,  $\eta = 1$ ,  $\epsilon = 0.1$ ,  $\sigma = 0.9$ , and the rest of the parameters are the same as in Section VI-A. The iteration process of the Stackelberg game is shown in Fig. 9. The game converges after 11 stages, in which  $\Delta_{\min} = r_{\max} - r_3 = 3 - r_3$  and gradually approaches 0. The first six stages undergo a constant price decrement ( $\phi = 5$ ), i.e.,  $M = 55, 50, 45, 40, 35, 30$  until  $\Delta_{\min} \leq \eta = 1$  is detected. After the CSMA subgame converges under the price  $M = 30$ , we have  $\Delta_{\min} = r_{\max} - r_3^* = 3 - 2.4 = 0.6$  and hence  $0.1 = \epsilon < \Delta_{\min} < \eta$ . Therefore, the Stackelberg game enters the second pricing phase, which consists of five stages ( $M = 27.10, 25.00, 23.68, 22.73, 22.12$ ), according to (33). We consider the game converged when  $\Delta_{\min} \approx 0.08 < \epsilon$ , and the optimal price is  $M^{\text{opt}} = 22.12$ . After convergence, the average

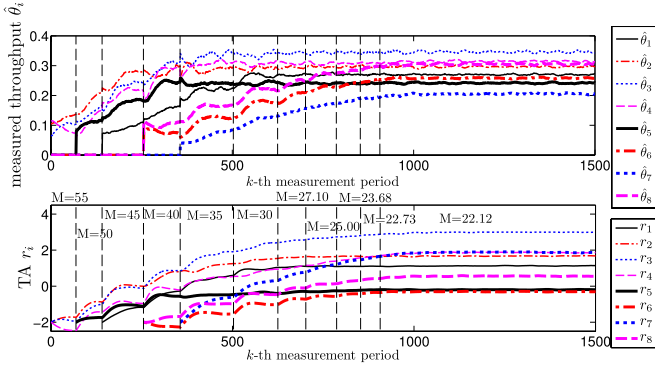


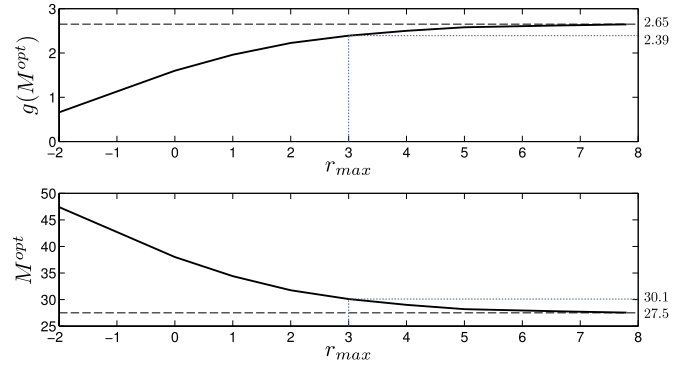
Fig. 9. Stackelberg games of the eight D2D links.

error of the measured throughputs, as compared with the target rates, is around  $\xi = 1\%$ . Notice that we cannot decrease  $M$  any further since the network is already close to the capacity boundary ( $r_3^* = 2.92 \approx r_{\max} = 3$ ). In other words, any further decrease in  $M$  would drive the target rate  $\tilde{\theta}$  outside the capacity region, and some D2D links (e.g., link 3) can no longer achieve their target rates. In summary, the proposed Stackelberg game is able to maximize the total throughput of the CSMA users, while the target rates of the heterogeneous users can all be satisfied.

The number of required stages before convergence is consistent with the analysis in Section V-E. In these simulations, the maximum value of the price is  $M_{\max} = 60$ , and the constant step  $\phi = 5$ . Therefore, the maximum number of stages in phase 1 is  $\lceil M_{\max}/\phi \rceil = 12$  or 6 on average. In the simulations, phase 1 actually consists of six stages before entering phase 2. In phase 2, the required precision  $\epsilon = 0.1$ ,  $\eta = 1$ , and the required number of stages is  $O(d \log_{10}(\eta/\epsilon))$ , where  $d = 1/(\log_{10} 1/(1 - \beta B))$ . The value of  $B$  can be estimated by using  $(\Delta_{\min}^{(l+1)} - \Delta_{\min}^{(l)})/(M^{(l+1)} - M^{(l)})$ , which is approximately 0.07 in the small interval  $\epsilon < \Delta_{\min} \leq \eta$ . Since we have chosen  $\beta = 5$ , hence  $0 < \beta B = 0.35 < 1$  and  $d = 1/(\log_{10} 1/(1 - \beta B)) = 5.3$ , and the required stages in phase 2 are on the order of a fixed multiple of  $d \log_{10}(\eta/\epsilon) = 5.3$ . In the simulations, phase 1 actually consists of five stages before convergence. Note that a smaller  $\beta$  could be used to guarantee  $\beta B < 1$ ; however, it also increases  $d$  and hence requires more stages for convergence. Finally, the total number of iterations required in the Stackelberg game is  $O(1/\xi) \cdot (O(1/\phi) + O(d \log_{10}(\eta/\epsilon)))$ , which is on the order of  $100 \cdot (6 + 5.3) = 1130$ . In the simulations, the Stackelberg game actually converges in around 1000 iterations, which is on the same order as the previous prediction.

### C. Effect of Parameter $r_{\max}$

In these simulations, we have used parameter  $r_{\max} = 3$  and obtained the optimal price  $M^{\text{opt}}$  that maximizes the total throughput  $g(M)$  for the eight users in Fig. 7 with heterogeneous rate requirements. As discussed at the end of Section V-B, by introducing the  $r_{\max}$  constraint, the feasible throughput region will shrink into a subset of the original one. Here, we apply different values of  $r_{\max}$  to the network and obtain the optimal price  $M^{\text{opt}}$  that maximizes the total throughput  $g(M)$  for the eight users in Fig. 7(a). To see the effect of parameter  $r_{\max}$  only, we assume

Fig. 10. Effect of parameter  $r_{\max}$ .

that the eight users are homogeneous in their rate requirements, i.e.,  $\gamma_i = 0.05$ ,  $\pi_i = 0.55$ ,  $b_i = 0.0125$ , and  $m_i = 50 \forall i \in \mathcal{N}$ .

The optimal price  $M^{\text{opt}}$  and the corresponding total throughput  $g(M^{\text{opt}})$  under each value of parameter  $r_{\max}$  are plotted in Fig. 10. In Fig. 10, we can see that, as the value of  $r_{\max}$  increases, the achievable total throughput  $g(M^{\text{opt}})$  also increases; moreover, the rate of increase gradually slows down. Recall that  $r_{\max}$  is used to refrain the D2D links from transmitting too aggressively. The outcome of introducing such a restriction is that the feasible throughput region will shrink into a subset of the original one. In particular, when  $r_{\max} = 3$ , the achievable total throughput is 2.39. For  $r_{\max} > 3$ , the total throughput curve becomes almost flat and approaches the upper bound 2.65 when  $r_{\max}$  tends to infinity (each user achieves a throughput of 0.33), under which the shrunk capacity region stretches back to the original feasible throughput region  $\bar{\mathcal{C}}$ . The corresponding bound on the optimal price is  $M^{\text{opt}} = 27.5$ . In other words, we cannot further reduce the price  $M$  below 27.5 to increase the target rate  $\tilde{\theta}$ , as it is already on the boundary of the feasible throughput region  $\bar{\mathcal{C}}$ .

It is observed in Fig. 10 that a larger  $r_{\max}$  value leads to a larger capacity region, but this also allows for longer transmission duration periods. However, the transmission duration should not be too long in practice; otherwise, it would lead to large access delay (where the access delay refers to the time between the onset of two consecutive successful transmissions of a link) and large variations of the delay. See [23, Sec. IV] for more discussions. As a result of these observations, we have adopted  $r_{\max} = 3$  in the previous two sections.

### D. Unstable Network Behavior Without Price Control From BS

Finally, we show the outcome of the CSMA game when there is no price control from the BS and when the collective target rates are outside the feasible throughput region  $\bar{\mathcal{C}}$  (corresponding to  $r_{\max} = +\infty$ ). Suppose the eight users in Fig. 7(a) all desire a target rate of 0.5 (which is larger than the upper bound 0.33 achieved by the Stackelberg game in Section VI-C), and they choose their TAs as in (28) to achieve their own target rates. The behaviors of the D2D links are plotted in Fig. 11. Since the target rates are not achievable even when  $r_{\max} = +\infty$ , each selfish user chooses an ever-increasing TA when its throughput is below its own target rate. When the TAs are high



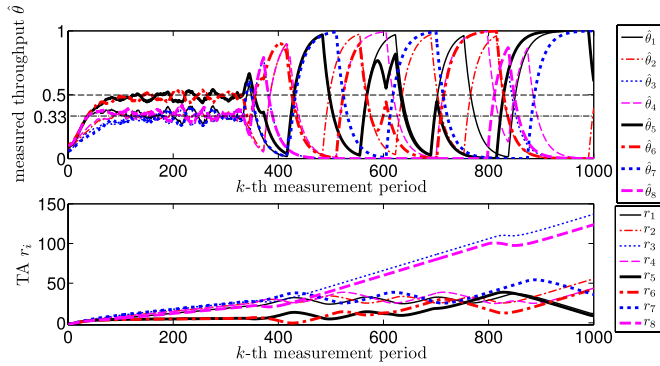


Fig. 11. Unstable network behavior without price control from BS.

enough, the users intermittently capture the whole channel and prevent their neighbors from transmitting for a long time, which results in unstable network behaviors and large access delay. On the other hand, with the pricing mechanism, the network is stable and the maximum total throughput  $g(M^{\text{opt}})$  is achieved as in Fig. 10, according to the  $r_{\text{max}}$  value chosen. Therefore, the BS plays an important role in tuning the service price so that the network always operates within the feasible throughput region.

## VII. CONCLUSION AND FUTURE WORK

We have studied a group of D2D links that shares a dedicated in-band overlay channel via CSMA. The ICN model is leveraged to analyze their behaviors and interactions under spatial reuse. We further assume that the D2D links have heterogeneous rate requirements and different willingness to pay, and they act nonaltruistically to achieve their target rates and maximize their own payoffs. To manage such noncooperative user dynamics, we propose a Stackelberg game in which the BS in the cellular network acts as a Stackelberg leader to regulate the D2D link transmissions by modifying the service price so that the total throughput is maximized while the heterogeneous target rates of the D2D links can all be satisfied. The problem is shown to be quasi-convex and can be solved by a sequence of equivalent convex optimization problems. The pricing strategies are designed so that the network always operates within the capacity region. The results are verified by simulations. The joint optimization of D2D link scheduling and cellular data offloading is our future work.

## REFERENCES

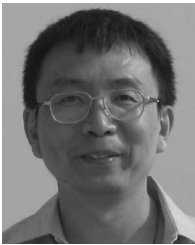
- [1] A. Asadi, Q. Wang, and V. Mancuso, "A survey on device-to-device communication in cellular networks," *IEEE Commun. Surveys Tuts.*, vol. 16, no. 4, 2014.
- [2] X. Lin, J. Andrews, and A. Ghosh, "Spectrum sharing for device-to-device communication in cellular networks," *IEEE Trans. Wireless Commun.*, vol. 13, no. 12, pp. 6727–6740, Dec. 2014.
- [3] S.-C. Liew, C. H. Kai, H. C. Leung, and P. Wong, "Back-of-the-envelope computation of throughput distributions in CSMA wireless networks," *IEEE Trans. Mobile Comput.*, vol. 9, no. 9, pp. 1319–1331, Sep. 2010.
- [4] S. Basagni, M. Conti, S. Giordano, and I. Stojmenovic, *Mobile Ad Hoc Networking*. Hoboken, NJ, USA: Wiley, 2004.
- [5] Y. Zhang, S. He, and J. Chen, "Data gathering optimization by dynamic sensing and routing in rechargeable sensor networks," *IEEE/ACM Trans. Netw.*, DOI: 10.1109/TNET.2015.2425146, to be published.
- [6] G. Bianchi, "Performance analysis of the IEEE 802.11 distributed coordination function," *IEEE J. Sel. Areas Commun.*, vol. 18, no. 3, pp. 535–547, Mar. 2000.
- [7] K. Ghaboosi, B. H. Khalaj, Y. Xiao, and M. Latva-aho, "Modeling IEEE 802.11 DCF using parallel space-time Markov chain," *IEEE Trans. Veh. Technol.*, vol. 57, no. 4, pp. 2404–2413, Jul. 2008.
- [8] I. Tinnirello, G. Bianchi, and Y. Xiao, "Refinements on IEEE 802.11 distributed coordination function modeling approaches," *IEEE Trans. Veh. Technol.*, vol. 59, no. 3, pp. 1055–1067, Mar. 2010.
- [9] R. Boorstyn, A. Kershenbaum, B. Maglaris, and V. Sahin, "Throughput analysis in multihop CSMA packet radio networks," *IEEE Trans. Commun.*, vol. 35, no. 3, pp. 267–274, Mar. 1987.
- [10] X. Wang and K. Kar, "Throughput modeling and fairness issues in CSMA/CA based ad-hoc networks," in *Proc. IEEE Conf. INFOCOM*, Miami, FL, USA, Mar. 2005, vol. 1, pp. 23–34.
- [11] L. Jiang and J. Walrand, "A distributed CSMA algorithm for throughput and utility maximization in wireless networks," *IEEE/ACM Trans. Netw.*, vol. 18, no. 3, pp. 960–972, Jun. 2010.
- [12] D. Fudenberg and J. Tirole, *Game Theory*. Cambridge, U.K.: MIT Press, 1993.
- [13] L. Song, D. Niyato, Z. Han, and E. Hossain, "Game-theoretic resource allocation methods for device-to-device communication," *IEEE Wireless Commun.*, vol. 21, no. 3, pp. 136–144, Jun. 2014.
- [14] Y. Cai, H. Chen, D. Wu, W. Yang, and L. Zhou, "A distributed resource management scheme for D2D communications based on coalition formation game," in *Proc. IEEE ICC*, Sydney, Australia, Jun. 2014, pp. 355–359.
- [15] D. Wu, J. Wang, R. Hu, Y. Cai, and L. Zhou, "Energy-efficient resource sharing for mobile device-to-device multimedia communications," *IEEE Trans. Veh. Technol.*, vol. 63, no. 5, pp. 2093–2103, Jun. 2014.
- [16] M. Ghazvini, N. Movahedinia, K. Jamshidi, and N. Moghim, "Game theory applications in CSMA methods," *IEEE Commun. Surveys Tuts.*, vol. 15, no. 3, pp. 1062–1087, 2013.
- [17] Y. Jin and G. Kesidis, "Distributed contention window control for selfish users in IEEE 802.11 wireless LANs," *IEEE J. Sel. Areas Commun.*, vol. 25, no. 6, pp. 1113–1123, Aug. 2007.
- [18] M. Cagalj, S. Ganeriwal, I. Aad, and J.-P. Hubaux, "On selfish behavior in CSMA/CA networks," in *Proc. IEEE Conf. INFOCOM*, Miami, FL, USA, Mar. 2005, vol. 4, pp. 2513–2524.
- [19] D. Kuptsov, B. Nechaev, A. Lukyanenko, and A. Gurtov, "How penalty leads to improvement: A measurement study of wireless backoff in IEEE 802.11 networks," *Comput. Netw.*, vol. 75, Part A, pp. 37–57, Dec. 2014.
- [20] L. B. Jiang and S. C. Liew, "Hidden-node removal and its application in cellular WiFi networks," *IEEE Trans. Veh. Technol.*, vol. 56, no. 5, pp. 2641–2654, Sep. 2007.
- [21] L. Fu, S. C. Liew, and J. Huang, "Effective carrier sensing in CSMA networks under cumulative interference," *IEEE Trans. Mobile Comput.*, vol. 12, no. 4, pp. 748–760, Apr. 2013.
- [22] J. Lyu, Y. H. Chew, and W.-C. Wong, "Aloha games with spatial reuse," *IEEE Trans. Wireless Commun.*, vol. 12, no. 8, pp. 3932–3941, Aug. 2013.
- [23] L. Jiang and J. Walrand, "Approaching throughput-optimality in distributed CSMA scheduling algorithms with collisions," *IEEE/ACM Trans. Netw.*, vol. 19, no. 3, pp. 816–829, Jun. 2011.
- [24] S. Boyd and L. Vandenberghe, *Convex Optimization*. New York, NY, USA: Cambridge Univ. Press, 2004.
- [25] L. Jiang, D. Shah, J. Shin, and J. Walrand, "Distributed random access algorithm: Scheduling and congestion control," *IEEE Trans. Inf. Theory*, vol. 56, no. 12, pp. 6182–6207, Dec. 2010.
- [26] M. J. Wainwright and M. I. Jordan, "Graphical models, exponential families, and variational inference," *Found. Trends Mach. Learn.*, vol. 1, no. 1/2, pp. 1–305, Jan. 2008.
- [27] Y. Jin and G. Kesidis, "A pricing strategy for an ALOHA network of heterogeneous users with inelastic bandwidth requirements," in *Proc. CISS*, Princeton, NJ, USA, Mar. 2002, pp. 1–4.
- [28] S. Boyd, L. Xiao, and A. Mutapic, "Subgradient methods," in *Lecture Notes of EE392o*. Stanford, CA, USA: Stanford Univ., Autumn Quart., 2003.
- [29] R. Amir and I. Grilo, "Stackelberg versus Cournot equilibrium," *Games Econ. Behav.*, vol. 26, no. 1, pp. 1–21, 1999.
- [30] M. S. Bazaraa, H. D. Sherali, and C. M. Shetty, *Nonlinear Programming: Theory and Algorithms*. New York, NY, USA: Wiley-Interscience, May 2006.
- [31] B. T. Polyak, *Introduction to Optimization*. New York, NY, USA: Optim. Softw., 1987.
- [32] Y. Nesterov, *Introductory Lectures on Convex Optimization*. Berlin, Germany: Springer-Verlag, 2004.



**Jiangbin Lyu** received the B.Eng. degree (Honors) in control science and engineering and completed the Chu Kochen Honors Program with Zhejiang University, Hangzhou, China, in 2011 and received the Ph.D. degree from NUS Graduate School for Integrative Sciences and Engineering (NGS), National University of Singapore (NUS), Singapore, in 2015 under the NGS scholarship.

He is currently a Postdoctoral Research Fellow with the Communications and Networks Laboratory, Department of Electrical and Computer Engineering, NUS, where he uses game theory, control theory, and optimization techniques to design stable and efficient communication systems, particularly in the subfields of device-to-device communication, cloud radio access networks, and cross-layer network optimization.

Dr. Lyu received the Best Paper Award at Singapore-Japan International Workshop on Smart Wireless Communications in 2014.



**Yong Huat Chew** (M'97) received the B.Eng., M.Eng., and Ph.D. degrees from the National University of Singapore (NUS), Singapore, all in electrical engineering.

Since 1996, he has been with the Institute for Infocomm Research (I<sup>2</sup>R, formerly also known as the Centre for Wireless Communications, NUS and Institute for Communications Research), which is an institute under the Agency for Science, Technology and Research, Singapore, where he is currently a Senior Scientist. From 1999 to June 2013, he was also

an Adjunct Faculty Member with the Department of Electrical and Computer Engineering, NUS. His research interests are in technologies related to high spectrally efficient wireless communication systems.



**Wai-Choong Wong** (S'76–M'77–SM'93) received the B.Sc. (First-Class Honors) and Ph.D. degrees in electronic and electrical engineering from Loughborough University, Loughborough, U.K., in 1976 and 1980, respectively.

From 1980 to 1983, he was a Member of the Technical Staff with Crawford Hill Laboratory, AT&T Bell Laboratories, Holmdel, NJ, USA. From November 2002 to November 2006, he was an Executive Director of the Institute for Infocomm Research (I<sup>2</sup>R), Agency for Science, Technology and

Research. He is currently a Professor with the Department of Electrical and Computer Engineering and the Deputy Director of the Interactive and Digital Media Institute, National University of Singapore (NUS), Singapore. Since joining NUS in 1983, he has been serving in various positions at the department, faculty, and university levels, including Head of the Department of Electrical and Computer Engineering from January 2008 to October 2009, Director of the NUS Computer Centre from July 2000 to November 2002, and Director of the Centre for Instructional Technology from January 1998 to June 2000. He is a coauthor of the book titled *Source-Matched Mobile Communications*. His research interests include wireless and sensor networks, ambient intelligent platforms, multimedia networks, and source matched transmission techniques with more than 250 publications and four patents in these areas.

Prof. Wong received the IEEE Marconi Premium Award in 1989; the NUS Teaching Award in 1989; the IEEE 3rd Millennium Award in 2000; the e-innovator Awards 2000, Open Category; and the Best Paper Award at the IEEE International Conference on Multimedia and Expo in 2006.